

**PCT**WORLD INTELLECTUAL PROPERTY ORGANIZATION  
International Bureau

## INTERNATIONAL APPLICATION PUBLISHED UNDER THE PATENT COOPERATION TREATY (PCT)

<b>(51) International Patent Classification <sup>6</sup> :</b> <b>G01R 33/28</b>	<b>A1</b>	<b>(11) International Publication Number:</b> <b>WO 99/53332</b> <b>(43) International Publication Date:</b> 21 October 1999 (21.10.99)
<b>(21) International Application Number:</b> PCT/GB99/01095 <b>(22) International Filing Date:</b> 9 April 1999 (09.04.99) <b>(30) Priority Data:</b> 9807879.3 9 April 1998 (09.04.98) GB <b>(71)(72) Applicants and Inventors:</b> WEILER, Norbert [DE/DE]; Geisberger Ring 21, D-67697 Otterberg (DE). DENINGER, Anselm [DE/DE]; Langendellschlag 70, D-65199 Wiesbaden (DE). EBERLE, Balthasar [DE/DE]; An der Selz 4a, D-55278 Hahnheim (DE). EBERT, Michael [DE/DE]; Staffelweg 4, D-55286 Wörrstadt (DE). GROSSMAN, Tino [DE/DE]; Freiherr von Stein Strasse 28, D-55131 Mainz (DE). HEIL, Werner [DE/FR]; La Giraudière, F-38760 Varcès-Alliers et Risset (FR). KAUCZOR, Hans-Ulrich [DE/DE]; Kirchbachstrasse 24, D-65191 Wiesbaden (DE). LAUER, Lars [DE/DE]; Dr.-Karl-Schramm-Strasse 2, D-55129 Mainz (DE). MARKSTALLER, Klaus [DE/DE]; Hochstrasse 4, D-55218 Ingelheim (DE). ROBERTS, Timothy [GB/US]; 1371 4th Avenue, San Francisco, CA 94122 (US). SCHREIBER, Wolfgang [DE/DE]; Trajanstrasse 16, D-55131 Mainz (DE). SURKAU, Reinhard [DE/DE]; Willi-Wolf-Strasse 22, D-55128 Mainz (DE).		<b>(74) Agents:</b> COCKBAIN, Julian et al.; Frank B. Dehn & Co., 179 Queen Victoria Street, London EC4V 4EL (GB). <b>(81) Designated States:</b> AE, AL, AM, AT, AT (Utility model), AU, AZ, BA, BB, BG, BR, BY, CA, CH, CN, CU, CZ, CZ (Utility model), DE, DE (Utility model), DK, DK (Utility model), EE, EE (Utility model), ES, FI, FI (Utility model), GB, GD, GE, GH, GM, HR, HU, ID, IL, IS, JP, KE, KG, KP, KR, KZ, LC, LK, LR, LS, LT, LU, LV, MD, MG, MK, MN, MW, MX, NO, NZ, PL, PT, RO, RU, SD, SE, SG, SI, SK, SK (Utility model), SL, TJ, TM, TR, TT, UA, UG, US, UZ, VN, YU, ZA, ZW, ARIPO patent (GH, GM, KE, LS, MW, SD, SL, SZ, UG, ZW), Eurasian patent (AM, AZ, BY, KG, KZ, MD, RU, TJ, TM), European patent (AT, BE, CH, CY, DE, DK, ES, FI, FR, GB, GR, IE, IT, LU, MC, NL, PT, SE), OAPI patent (BF, BJ, IN, CF, CG, CI, CM, GA, GN, GW, ML, MR, NE, SN, TD, TG). <b>Published</b> <i>With international search report. Before the expiration of the time limit for amending the claims and to be republished in the event of the receipt of amendments.</i>
<b>(54) Title:</b> USE OF A HYPERPOLARIZED GAS FOR MRI DETECTION OF REGIONAL VARIATIONS IN OXYGEN UPTAKE FROM THE LUNGS <b>(57) Abstract</b> <p>The invention provides a method of detecting regional variations in oxygen uptake from the lungs of an air-breathing animal subject, said method comprising administering into the lungs of said subject a diagnostically effective amount of a gaseous hyperpolarized magnetic resonance imaging agent, detecting the magnetic resonance signal from said agent in said lungs, determining the temporal variation in relaxation rate for said signal for at least one region of interest within said lungs, and from said variation generating a qualitative or quantitative value or image indicative of the oxygen concentration in at least one region of interest, and if desired the time dependency of such concentration.</p>		

**FOR THE PURPOSES OF INFORMATION ONLY**

Codes used to identify States party to the PCT on the front pages of pamphlets publishing international applications under the PCT.

AL	Albania	ES	Spain	LS	Lesotho	SI	Slovenia
AM	Armenia	FI	Finland	LT	Lithuania	SK	Slovakia
AT	Austria	FR	France	LU	Luxembourg	SN	Senegal
AU	Australia	GA	Gabon	LV	Larvia	SZ	Swaziland
AZ	Azerbaijan	GB	United Kingdom	MC	Monaco	TD	Chad
BA	Bosnia and Herzegovina	GE	Georgia	MD	Republic of Moldova	TG	Togo
BB	Barbados	GH	Ghana	MG	Madagascar	TJ	Tajikistan
BE	Belgium	GN	Guinea	MK	The former Yugoslav Republic of Macedonia	TM	Turkmenistan
BF	Burkina Faso	GR	Greece	ML	Mali	TR	Turkey
BG	Bulgaria	HU	Hungary	MN	Mongolia	TT	Trinidad and Tobago
RJ	Benin	IE	Ireland	MR	Mauritania	UA	Ukraine
BR	Brazil	IL	Israel	MW	Malawi	UG	Uganda
BY	Belarus	IS	Iceland	MX	Mexico	US	United States of America
CA	Canada	IT	Italy	NE	Niger	UZ	Uzbekistan
CF	Central African Republic	JP	Japan	NL	Netherlands	VN	Viet Nam
CG	Congo	KE	Kenya	NO	Norway	YU	Yugoslavia
CH	Switzerland	KG	Kyrgyzstan	NZ	New Zealand	ZW	Zimbabwe
CI	Côte d'Ivoire	KP	Democratic People's Republic of Korea	PL	Poland		
CM	Cameroon	KR	Republic of Korea	PT	Portugal		
CN	China	KZ	Kazakstan	RO	Romania		
CU	Cuba	LC	Saint Lucia	RU	Russian Federation		
CZ	Czech Republic	LI	Liechtenstein	SD	Sudan		
DE	Germany	LK	Sri Lanka	SE	Sweden		
DK	Denmark	LR	Liberia	SG	Singapore		
EE	Estonia						

**USE OF A HYPERPOLARIZED GAS FOR MRI DETECTION OF REGIONAL  
VARIATIONS IN OXYGEN UPTAKE FROM THE LUNGS**

5     Field of the Invention

          This invention relates to a method of magnetic  
resonance imaging of the human or animal (e.g.  
mammalian, reptilian or avian) body by which lung  
10    function and, if desired, morphology may be  
investigated. .

Background of the Invention

15           Lung function is of interest to physicians,  
especially when dealing with patients who may have  
abnormalities of ventilation or perfusion or other  
determinants of gas exchange in the lung. For proper  
lung function five conditions must be met:

- 20    1.   gas (air) must flow into and out of the lungs;  
      2.   the gas must be distributed evenly within the  
          lungs;  
      3.   gases must be exchanged by diffusion between the  
          blood and the alveolar space;  
25    4.   blood must be pumped through the lungs; and  
      5.   the distribution of the blood in the lungs should  
          match the distribution of gas in the alveolar space  
          (i.e. where the gas penetrates to, blood should flow).

30           All diseases and ailments relating to the lungs and  
airways affect one or more of the five conditions above.

          It has therefore been known to study lung  
ventilation and perfusion using various diagnostic  
techniques. The conventional technique is known as VQ  
imaging and involves the use of two different  
35    radiopharmaceuticals, one to study perfusion and the  
other to study ventilation.

          The perfusion agent is generally a particulate

- 2 -

(e.g.  $^{99m}\text{Tc}$ -macroaggregated albumin) which is administered intravenously upstream of the lungs and lodges in the precapillary arterioles.

5 Images are recorded with a gamma camera and the signal intensity may be used to detect local abnormalities in blood flow.

The ventilation agent is generally a radioactive gas or aerosol or microparticulate, e.g.  $^{133}\text{Xe}$ ,  $^{127}\text{Xe}$  or  $^{81m}\text{Kr}$ , or a  $^{99m}\text{Tc}$ -DTPA aerosol or  $^{99m}\text{Tc}$ -labelled carbon  
10 particles. The agent is inhaled and an image is recorded with a gamma camera. Signal intensity and distribution may be used to detect airway obstructions or regional abnormalities in ventilation.

Where there is a mismatch between the ventilation  
15 and perfusion images (which are generated at different times), various different lung malfunctions, diseases or abnormalities may be diagnosed, e.g. pulmonary embolism, pleural effusion/atelectasis, pneumonia, tumour/hilar adenopathy, pulmonary artery obstruction, AVM, CHF, and  
20 intravenous drug use. Heterogenous perfusion patterns may likewise be used to diagnose various disease states or disorders, e.g. CHF, lymphangitic carcinomatosis, non-thrombogenic emboli, vasculitis, chronic interstitial lung disease, and primary pulmonary  
25 hypertension. Decreased perfusion to one lung may be used to diagnose pulmonary embolism, pulmonary agenesis, hypoplastic lung (pulmonary artery stenosis), Swyer-James syndrome, pneumothorax, massive pleural effusion, tumour, pulmonary artery sarcoma and shunt procedures  
30 for congenital heart disease.

VQ imaging however involves exposing the patient to radiation doses from two radiopharmaceuticals in two temporally separate imaging procedures. Clearance of the injected particulate agent is relatively slow and  
35 the agent is taken up in other organs besides the lungs. Moreover, in patients with severe pulmonary hypertension, the injected particulate causes a risk of

- 3 -

acute right heart failure. For pregnant patients the radiation dose involved in VQ imaging results in undesirable levels of radiation exposure for the foetus.

Furthermore, for most diagnostic purposes mentioned  
5 above the resolution of conventional VQ imaging is unsatisfactory.

There is thus a need for a technique which permits lung function to be assessed without the drawbacks associated with VQ imaging.

10 In magnetic resonance (mr) imaging, radiofrequency signals from non-zero spin nuclei which have a non-equilibrium nuclear spin state distribution are detected and may be manipulated to provide images of the subject under study. In conventional mr imaging the nuclei  
15 responsible for the detected signals are protons (usually water protons) and the non-equilibrium spin state distribution is achieved by placing the subject in a strong magnetic field (to enhance the population difference between the proton spin states at  
20 equilibrium) and by exposing the subject to pulses of rf radiation at the proton Larmor frequency to excite spin state transitions and create a non-equilibrium spin state distribution. However the maximum deviation from equilibrium is that achievable by spin state population  
25 inversion and, since the energy level difference between ground and excited states is small at the temperatures and magnetic field strengths accessible, the signal strength is inherently weak.

An alternative approach that has been developed is  
30 to "hyperpolarize" (i.e. obtain a nuclear spin state population difference greater than the equilibrium population difference) an imaging agent containing non-zero nuclear spin nuclei (e.g. by optical pumping, by polarization transfer or by subjecting such nuclei ex  
35 vivo to much higher magnetic fields than those used in the mr imaging apparatus), to administer the hyperpolarized agent to the subject, and to detect the

- 4 -

mr signals from the hyperpolarized nuclei as they relax back to equilibrium. In this hyperpolarized mr imaging technique, described for example in W095/27438, the hyperpolarized material is conveniently in gaseous form, e.g.  $^3\text{He}$  or  $^{129}\text{Xe}$ , and it may thereby be administered by inhalation into the lung and the mr signal detected may be used to generate a morphological image of the lungs.

Since the relaxation time  $T_1$  for  $^3\text{He}$  in the lungs is about 10 seconds it is feasible, using fast imaging techniques, to generate a morphological image of the lungs from the  $^3\text{He}$  signal following inhalation of hyperpolarized  $^3\text{He}$  gas and at any desired stage of the breathing cycle, e.g. during breathhold. Since the mr signal selected is from the  $^3\text{He}$  atoms and since the helium is in the gas phase in the lungs, the image detected is essentially only of the airways into and within the lungs. By administering the hyperpolarized agent as a bolus followed or preceded by other gases or aerosols, e.g. by air, nitrogen or  $^4\text{He}$ , the hyperpolarized agent can be positioned at any desired section of the airways or other aerated spaces in the body, e.g. it may be flushed from the trachibronchial tree and the image generated is then essentially only of the alveolar space.

We have now found that functional imaging of the lungs may be carried out effectively using mr imaging of an inhaled hyperpolarized agent by making use of the variation with time of the relaxation rate  $T_1$  of the hyperpolarized agent in conjunction with imaging of the regional and temporal distribution of ventilation using hyperpolarized gases.

#### Summary of the Invention

Viewed from one aspect therefore, the invention provides a method of detecting regional variations in oxygen uptake from the lungs of an air-breathing animal

- 5 -

subject, e.g. a mammalian (human or non-human), avian or reptilian subject, said method comprising administering into the lungs of said subject a diagnostically effective amount of a gaseous hyperpolarized magnetic resonance imaging agent, detecting the magnetic resonance signal from said agent in said lungs, determining the temporal variation in relaxation rate (e.g.  $T_1$  relaxation rate) for said signal for at least one region of interest within said lungs, and from said variation generating a qualitative or quantitative value or image indicative of the oxygen concentration in the alveolar space in said at least one region of interest, and if desired the time dependency of such concentration as a result for example of physiological process, e.g. oxygen uptake by perfusion.

In a preferred embodiment, the method of the invention also involves generation of a temporal and/or spatial image of the distribution of the hyperpolarized agent in at least part of the lungs of the subject, preferably in the alveolar space within the lungs.

In a further preferred embodiment, the method also involves generation of a magnetic resonance image of at least part of the lungs of the subject following administration into the subject's vasculature of a second mr agent, preferably an agent which affects proton relaxation (with the image generated being a proton mr image) or more preferably an agent containing non-proton mr active nuclei (e.g.  $^{19}\text{F}$ ,  $^{13}\text{C}$ ,  $^{31}\text{P}$ ,  $^{17}\text{O}$ , etc.) in which case the mr image will be generated from mr signals from such non-proton mr active nuclei. The mr active nuclei in the second agent will preferably not be the same as those in the hyperpolarized agent unless the image generated using the second agent is generated at a time when the lungs contain substantially none of the hyperpolarized agent.

Lung volume may also be estimated from the integrated  $^3\text{He}$  mr signal (or by  $^3\text{He}$  mrs) following

- 6 -

inhalation of the  $^3\text{He}$  without air, breathhold, and expiration where the expired volume is measured directly and the residual hyperpolarization of the retained  $^3\text{He}$  is extrapolated from the hyperpolarization value (signal strength) monitored during breathhold.

In the method of the invention, it is preferred that for at least part of the mr signal detection period (preferably at least 1 second, more preferably at least 5 seconds, still more preferably at least 10 seconds, e.g. 20 sec to 1 minute), there be substantially no flow of gas into or out of the lungs, e.g. that there should be a breathhold period, and that the indication of oxygen uptake be derived from mr signals detected during at least part of this period. However, in a preferred embodiment, the method of the invention will also involve mr signal detection during gas flow into and/or out of the lungs with or without a period of breathhold. In this way, spatial or temporal images or other indications of lung ventilation may be generated from the detected mr signals.

Because the detected mr signal derives from the hyperpolarized agent, the signal strength is effectively independent of the primary field strength of the magnet in the mr imager. Accordingly low or high field, e.g. 0.05 to 3.5T, machines may be used.

#### Description of the Drawings

The method of the invention is illustrated by the attached drawings, in which:

Figures 1a and 1b show  $^3\text{He}$  mr images showing the effect of oxygen and flip angle on the images obtained using a 40 mL bolus of  $^3\text{He}$ ;

Figure 2 shows  $^3\text{He}$  mr images of the airway;

Figure 3 shows the  $^3\text{He}$  mr signal strength in the trachea during inspiration and breathhold where a bolus of  $^3\text{He}$  is estimated;



- 7 -

Figure 4 shows a plot of regional  $F_{ip}O_2$  against  $F_{et}O_2$  (see Example 7);

Figure 5 shows a plot of  $F_{ip}O_2$  versus time (see Example 7);

5        Figure 6 shows a plot of  $D_n$  against number of images (see Example 3);

Figure 7 shows a plot of signal intensity evolution (see Example 3);

10       Figure 8 shows a plot of signal against number of images (see Example 3);

Figure 9 shows a plot of signal intensities as a function of time (see Example 5);

Figure 10 shows a plot of  $pO_2$  versus time (see Example 6);

15       Figure 11 shows images from a healthy volunteer after inspiration of a single bolus (see Example 9); and

Figure 12 shows a plot of signal versus time (see Example 9).

20       Detailed description of the Invention

The method of the invention involves administration of a gaseous hyperpolarized mr agent. By a gaseous agent is meant a gas as such (e.g.  $^3\text{He}$  or  $^{129}\text{Xe}$ ) or a  
25       particulate agent held in the gas phase, e.g. an aerosol of powder or droplets. In the latter case, the gaseous carrier preferably is substantially free of paramagnetic gases such as oxygen. The hyperpolarized agent will conveniently have a polarization degree  $P$  of 2 to 75%,  
30       e.g. 10 to 50%. The mr active (i.e. non-zero nuclear spin) nuclei which are hyperpolarized may be any mr active nuclei which can be hyperpolarized and which can be presented in a gaseous form (i.e. elemental or molecular form, e.g.  $\text{SF}_6$ ) which is physiologically  
35       tolerable. Examples of appropriate nuclei include various noble gas, carbon, nitrogen and fluorine isotopes; however the noble gases, e.g. He and Xe, and

- 8 -

most especially  $^3\text{He}$ , are the most preferred. Accordingly, the discussion below will present the invention in terms of  $^3\text{He}$ -mr imaging although it does as indicated above, extend to cover the use of other mr active nuclei.

During steady state, oxygen transport within the functional units of the lung, i.e. the alveolocapillary unit is characterized by a relationship governed by mass conservation:

The net amount of oxygen entering the alveolocapillary unit by the airways has to be equal to the net amount of oxygen leaving the alveolocapillary unit on the blood side. This may be expressed by the equation:

$$V' \cdot (F_{\text{I}}\text{O}_2 - F_{\text{E}}\text{O}_2) = Q \cdot (c_{\text{a}}\text{O}_2 - c_{\text{v}}\text{O}_2) \quad (1)$$

$V'$  = ventilation

$Q$  = perfusion

$F_{\text{I}}\text{O}_2$  = fractional inspiratory concentration of oxygen

$F_{\text{E}}\text{O}_2$  = fractional expiratory concentration of oxygen

$c_{\text{a}}\text{O}_2$  = oxygen content of arterial blood

$c_{\text{v}}\text{O}_2$  = oxygen content of mixed venous blood

Rearrangement of equation (1) provides the following equation for the ventilation-perfusion ratio  $V'/Q$ :

$$\frac{V'}{Q} = \frac{c_{\text{a}}\text{O}_2 - c_{\text{v}}\text{O}_2}{F_{\text{I}}\text{O}_2 - F_{\text{E}}\text{O}_2} \quad (2)$$

Oxygen contents as well as fractional oxygen concentrations can both be written as functions of oxygen partial pressure, yielding the following equation:

$$\frac{V'}{Q} = \frac{k(p_{\text{a}}\text{O}_2 - p_{\text{v}}\text{O}_2)}{F_{\text{I}}\text{O}_2 - F_{\text{E}}\text{O}_2} + f(p_{\text{a}}\text{O}_2 - p_{\text{v}}\text{O}_2) \quad (3)$$

- 9 -

$$Q \quad (p_{I}O_2 - p_{E}O_2)$$

Assuming complete equilibration of oxygen partial pressures across the alveolocapillary membrane,  $p_aO_2$  will be equal to  $p_EO_2$ :

$$\frac{V'}{Q} = \frac{k(p_{E}O_2 - p_{V}O_2)}{(p_{I}O_2 - p_{E}O_2)} + f(p_aO_2 - p_{V}O_2) \quad (4)$$

Both  $k$  and  $f$  depend on a variety of factors, e.g. on barometric pressure, the solubility constant of oxygen in plasma, the dissociation curve of oxygenated haemoglobin, etc., all of which are known.

Until now, quantitative description of these oxygen transport processes was possible only on a global basis for the whole organism.

With the present invention one is able to measure these processes regionally in the lung. The method may be used to measure regional ventilation, regional partial pressure of oxygen and its time course, with high spatial and temporal resolution.

Regional oxygen partial pressure may be measured by hyperpolarized gas magnetic resonance imaging, e.g. hyperpolarised  $^3\text{He}$  gas magnetic resonance imaging.

To this end, ultrafast MRI sequences are preferably used allowing sequential measurements of the  $^3\text{He}$  signal, and its decay, which is dependent both on oxygen and MR acquisition (see Figures 1 a and b). Signal decay induced by the MR sequence is corrected for by variation of the flip angle and/or of the inter-scan delay.

Oxygen concentration inspired into the alveolocapillary unit is not constant during a single inspiration, due to the contribution of deadspace. Therefore, mean inspiratory concentration may be calculated based upon determination of deadspace (from airway imaging by  $^3\text{He}$ ; see Figure 2), and from the inspiratory concentration administered at the mouth.

- 10 -

Regional ventilation may be measured by quantitative analysis of temporal changes in hyperpolarization signal in the trachea, and parallel to this, in the alveolar space, following inspiration of a single bolus of hyperpolarized gas. This analysis is performed on the basis of a mass balance, which allows the determination of functional residual capacity and serial deadspace on a global and regional basis. These signal changes can be measured over several respiratory cycles by ultrafast pulse sequences (e.g., temporal resolution <150 ms) and flow flip angles (Fig. 2 and 3).

Knowing intraalveolar oxygen partial pressure and mean inspiratory oxygen partial pressure, the local  $V'/Q$  ratio can be calculated; the addition of local ventilation then allows calculation of regional perfusion. With the assumption that local arterial  $pO_2$  equals alveolar  $pO_2$ , local oxygen uptake can be derived. Thus, for the first time, a complete status of regional oxygen transport in the lung can be obtained.

The preferred MRI sequences for use in the method of the invention are:

- for oxygen partial pressure determination, short repetition time gradient-recalled echo sequences with small flip angle; and
- for determination of ventilation, ultra-short repetition time (< 2 ms) gradient-recalled echo sequences with small flip angle, or echo-planar pulse sequences, or ultra-fast sequences using low flip angle and free induction decay.

The theory of  $^3\text{He}$ -MR-based on  $pO_2$  analysis will now be discussed briefly:

The decay of longitudinal magnetization, and hence signal intensity, that occurs with any mr acquisition, follows a function given by:

$$S_{n+1,a}(r) = S_n * \cos^a a \quad (5)$$

- 11 -

where  $n$  is the number of image acquisition,  $r$  is the number of radiofrequency impulses (lines) per image acquired, and  $a$  is the flip angle imposed by each consecutive radiofrequency impulse upon the nuclear spin polarization of  $^3\text{He}$  in the acquisition volume.

Simultaneously, signal intensity ( $S_n$ ) also begins to decay according to an exponential function, to arrive (within a given time interval  $Dt$ ) at  $S_{n+1}$ :

10

$$S_{n+1,Dt}(t) = S_n * \exp\{-Dt/T_1(t)\} \quad (6)$$

The time constant of this decay is determined by the longitudinal spin relaxation time of  $^3\text{He}$ ,  $T_1$ , which is shortened in the presence of paramagnetic molecular oxygen.

In *in vitro* experiments, the following relationship between  $T_1$  and oxygen concentration  $[\text{O}_2]$  in a gas mixture containing hyperpolarized  $^3\text{He}$  has already been established to be:

$$\begin{aligned} T_1(\text{O}_2) &= k/[\text{O}_2], \text{ where } k = 2.27 \text{ amagat}\cdot\text{s}; \\ &\text{at temperature } 37^\circ\text{C} \\ &(\text{T}_1 \text{ in seconds; } [\text{O}_2] \text{ in amagat; } 1 \text{ amagat} = \text{gas} \\ &\text{density } (2.68675 \times 10^{13} \text{ molecules per cm}^3)) \end{aligned} \quad (7)$$

The combined effects of acquisition and time result in a decay function of (valid for constant  $T_1$ ):

$$S_{n+1}(a,t) = S_n * \cos^r a * \exp\{-Dt/T_1\} \quad (8)$$

More generally, signal of image  $n$  acquired at time  $t_n$  ( $n = 0, 1, \dots, n_{\max}$ ) given by

$$S(t_n) = S_0 (\cos a)^{nr} \exp\left(-\int_0^{t_n} [\text{O}_2(t)] dt/k\right) \quad (8a)$$

Thus two values (flip angle  $a$  and oxygen

- 12 -

concentration  $[O_2(t)]$  have to be extracted from image intensities. Therefore make use of imaging with variation of one parameter, e.g. time interval  $\tau$  between images, or RF amplitude  $U_{RF}$ . This can be done either in  
5 two separate imaging experiments ("double acquisition") or within one experiment with a more intricate sequence (see attached examples). Thereby both values can be quantified simultaneously without additional input parameters.

10 Hyperpolarized helium-3 ( $^3\text{He}$ ) can be produced by means of direct optical pumping from the metastable state  $1s2s^3S_1$  at 1mb with subsequent conversion to convenient pressures of 1-6 bar. Surkau et al. in Nucl. Inst. & Meth. A384: 444-450 (1997) describe apparatus  
15 which can be used to produce  $^3\text{He}$  with a polarization degree  $P$  of at least 50% at a flow of  $3.5 \times 10^{18}$  atoms/sec. or 40% at a flow rate of  $8 \times 10^{18}$  atoms/sec. The hyperpolarized gas may then be filled into glass cylinders, e.g. made of glass which has a low iron  
20 content and no coating. These cylinders can be closed by a stop-cock and transported to the mr imaging site, preferably within a magnet, eg a 0.3mT magnet. Under such conditions, the  $^3\text{He}$  has a relaxation time ( $T_1$ ) of up to 70 hours.

25 To perform  $^3\text{He}$  mr imaging, the hyperpolarized gas is preferably administered in a bolus into an application unit through which the subject under study may breath freely or alternatively ventilation may be supported by artificial ventilation. For non-human subjects at  
30 least, artificial ventilation apparatus will preferably be used and the animals will preferably be anaesthetized and relaxed. For humans, with whom voluntary breathhold is feasible, free breathing through the ventilation unit will generally be preferred. In this way, the  $^3\text{He}$  bolus,  
35 conveniently of 1 to 1000ml, may be administered at a desired point within the breathing cycle, generally at or close to the beginning of inspiration. The bolus

- 13 -

size used will depend on the lung size or tidal respiration volume of the subject and will thus vary with subject size or species. However a bolus of 2 to 50%, preferably 5 to 25%, of tidal respiration volume  
5 may be suitable.

On inspiration the  $^3\text{He}$  bolus passes into the airways within about one second with alveolar filling occurring rapidly thereafter for healthy/unobstructed tissue. If inspiration is followed by a period (e.g. of 1 to 60  
10 seconds during which there is substantially no gas flow into or out of the lungs, e.g. a period of breathhold), the  $^3\text{He}$ -mr signal gradually decays at a relaxation rate of the order of 10 seconds. The relaxation rate however is not constant spatially or temporally. Three  
15 significant factors contribute to this: loss of polarization due to the magnetic field changes required for mr imaging; loss of polarization due to relaxation enhancement by gaseous oxygen present in the lungs; and loss of polarization due to relaxation enhancement by  
20 the tissue/gas boundary. If the same imaging sequence(s) is used throughout the signal detection period, then the first and third of these factors are constant during a period of no gas flow to/from the lungs; however,  $^3\text{He}$  filled volumes as well as oxygen  
25 concentration will vary due to physiological processes, e.g. as oxygen is taken up from the lungs in the alveolar space. As a result, in a region of interest where oxygen concentration drops the  $^3\text{He}$  relaxation time will increase with time even though absolute signal  
30 intensity will continue to drop.

While relaxation rate enhancement by lung tissue plays a subordinate role in terms of the overall contributions to the  $^3\text{He}$  relaxation rate, it does have a non-uniform effect as different tissues or abnormalities  
35 have different effects on the relaxation rate. It is thus preferred not to estimate the oxygen contribution to the relaxation rate by simple reference to a phantom

- 14 -

undergoing the same field gradient changes as the subject's lung. Use of a phantom is similarly non-preferred due to the inhomogeneity in the applied field across the volume in which the  $^3\text{He}$  distributes.

5 Accordingly it is preferred to extract the oxygen contribution to the relaxation rate by mr signal detection during at least two different types of signal generation, e.g. with the different sequences being interleaved. Thus for example the different sequences  
10 may involve different RF excitation intensities and/or different sequence intervals ( $\tau$ ).

The magnetic field change contribution to the relaxation is desirably minimized so as to prolong the period over which a signal with an acceptable signal to  
15 noise ratio can be detected. This is generally achieved by using small flip angles (e.g. less than  $7^\circ$ , preferably less than  $4^\circ$ ) in the imaging sequences and in this way mr signals may be detected for up to 60 seconds following bolus  $^3\text{He}$  administration.

20 For  $^3\text{He}$ -mr imaging, because of the relatively short duration of the hyperpolarization and because relaxation rate change over time is to be studied, it is of course appropriate to use rapid image generating techniques, e.g. fast gradient echo techniques or other techniques  
25 with an image acquisition time of less than 2 seconds, preferably 1 second or less. Such techniques are mentioned elsewhere in this specification. Images generated in this way may have a spatial resolution (i.e. voxel size) of less than  $20\text{ mm}^2$ , which is far  
30 superior to the scintigraphic ventilation images in conventional VQ imaging.

The regions of interest studied in the method of the invention will generally be the alveolar space and thus it is generally preferable that the  $^3\text{He}$  bolus be  
35 followed in the same gas intake by air or nitrogen to flush the  $^3\text{He}$  from the tracheobronchial tree and into the alveolar space.



- 15 -

As mentioned above, the method of the invention may, and probably will, involve generation of ventilation images, showing spatial and/or temporal distribution of  $^3\text{He}$ , thereby permitting ventilation and perfusion to be determined in the same imaging procedure (unlike VQ imaging). On a morphological level, such ventilation images may identify airway obstructions simply by identifying regions to which the  $^3\text{He}$  does not penetrate, penetrates slowly, or penetrates at lower than normal concentrations. Obstructions and associated hypoperfusion, normal perfusion or hyperperfusion can also be identified by following the time dependence of the  $^3\text{He}$  relaxation rate for slowly penetrated alveolar space as the oxygen concentration in such areas may be abnormally low or high. Thus while the mr signal strength may initially be abnormally low, the local relaxation rate may be or become abnormally high or low.

Thus if local perfusion does not match local ventilation, oxygen concentration in that part of the lung will be affected and measurable by the method of the invention due to the local abnormal relaxation rate. This would be important in the case of patients with lung malfunction due to smoking.

As also mentioned above,  $^3\text{He}$  mr imaging may be combined with perfusion imaging with or without administration of a contrast agent, using a second imaging agent administered into the vasculature, e.g. a blood pool agent such as a polymeric paramagnetic chelate, or a superparamagnetic agent or, more preferably because of its oxygen sensitivity, a  $^{19}\text{F}$  fluorocarbon emulsion. In the former cases, imaging would be proton mr imaging, in the latter case  $^{19}\text{F}$  mr imaging. However, the perfusion data collected in this way, although equivalent to the perfusion data collected in VQ imaging, is not absolutely equivalent to that generated in the method of the invention since the second imaging agent distribution merely identifies the

- 16 -

regions of the lung to which blood flows and not whether or not oxygen uptake by the blood occurs in such regions. Accordingly, the perfusion data from the method of the invention provides a more comprehensive  
5 portrayal of lung function.

The method of the invention may be used as part of a method of diagnosis of lung malfunction, disease, etc. or indeed in combination with a method of treatment to combat, i.e. prevent or cure or ameliorate, a lung  
10 malfunction or disease, etc., e.g. a method involving surgery or administration of therapeutic agents or a method of diagnosis of one of the lung malfunctions or diseases mentioned above. Such methods form further aspects of the present invention as does the use of  $^3\text{He}$   
15 (or other mr active nuclei containing materials) for the preparation of a hyperpolarized imaging agent for use in methods of treatment or diagnosis involving performance of the method of the invention.

All documents referred to herein are hereby  
20 incorporated by reference.

The invention will now be illustrated further by reference to the following non-limiting Examples:

#### Example 1

25

The objectives in this Example were to realize single-breath, single-bolus visualization of intrapulmonarily administered  $^3\text{He}$  to analyse nuclear spin relaxation of  $^3\text{He}$  *in vivo* and to determine the regional  
30 oxygen concentration, i.e.  $[\text{O}_2]$ , and its time dependent change by perfusion. A double acquisition technique is described which also permits estimation of regional gas transport.

In these examinations, the source of the MR signal  
35 is the large non-equilibrium polarization of  $^3\text{He}$ . This polarization is achieved by means of direct optical pumping from its metastable state  $1s2s^3S_1$  at 1mb with

- 17 -

subsequent compression to a convenient pressure of 1-6 bar. The apparatus is described by Surkau et al. Nuc. Instr. & Meth. A 384 (1997) 444-450 and is capable of yielding  $P > 50\%$  at flow of  $3.5 \times 10^{18}$  atoms/s and  $40\%$  at flow  $8 \times 10^{18}$  atoms/s. The gas is filled into glass cylinders with long relaxation times. Cylinders for medical application are made from "Supremax glass" with low iron content and no coating. They show relaxation times up to 70 h and can be closed by a stop cock and disflanged from the filling system. Transport from the filling site to the MR imaging unit takes place inside a dedicated 0.3 mT guiding field. To perform  $^3\text{He}$ -MRI experiments reproducibly, an application system was used. Predefined quantities of  $^3\text{He}$  gas at 1 bar pressure can be inserted into breath at a predefined position. Volunteers or patients can breathe freely through the application unit or ventilation can be supported by a commercial respiration machine with controlled pressure. For studies with anesthetized and relaxed animals ventilation is by a respiration machine.

Relaxation of the non-equilibrium polarization of inhaled  $^3\text{He}$  *in vivo* is mainly caused by NMR excitations and the presence of oxygen. Relaxation by lung tissue plays a subordinate role as shown by experiments below. The time evolution of the polarization  $P$  inside a two-dimensional partition inside ventilated lung spaces can be described by rate equations. Considering the flip angle  $\alpha$  and the partial oxygen pressure  $pO$  we define a time-averaged relaxation rate by NMR via the equation

30

$$\Gamma_{RF} = -n_{\max} r \ln(\cos \alpha) / T_{\text{tot}} \quad (12)$$

(where  $T_{\text{tot}}$  = duration of measurement,  $n_{\max}$  = index number of last image,  $r$  = number of NMR excitations per image) and by oxygen via the equation

- 18 -

$$\Gamma_1(O_2) = [O_2(t)]/k$$

k = 2.27 amagat\*s at temperature 37°C referring to 299  
 Kelvin [see Saam et al. in Phys. Rev. A 52 (1995)  
 862-865]. Since  $[O_2]$  changes in vivo by oxygen  
 consumption,  $[O_2]$  is taken as a function of time t. Gas  
 5 exchange from neighbouring volumes with polarization  $P'$ ,  
 e.g. by diffusion, is taken into account by an exchange  
 rate  $\gamma$ , weighted with the polarization difference ( $P -$   
 $P'$ ). Assuming only relaxation by oxygen and wall  
 contact for  $P'$ , the time dependence of  $P$  is integrated  
 10 to:

$$P_n = \frac{P_0}{\gamma + \Gamma_{RF}} \left\{ \Gamma_{RF} \exp(-\int_0^m \Gamma_{O_2}(t) dt) \exp(-(\Gamma_\omega + \gamma)m) (\cos \alpha)^{nN} + \gamma \exp(-\int_0^m \Gamma_{O_2}(t) dt) \exp(-\Gamma_\omega t_n) \right\}$$

Experiments have been carried out to investigate  
 the dependence of  $P(t)$  on the given parameters. Signal  
 intensities were averaged and analysed over regions of  
 15 interests (ROIs). Since signal to noise ratios were  
 always >3, an intensity correction for noise was  
 performed following the method of Gudbjartsson et al.,  
 MRM 34 (1995) 910-914. The noise corrected signals  $A_n$  of  
 the  $n^{th}$  image ( $n = 0, 1, \dots$ ) are proportional to  $P_n$ .  
 20 The data are normalized and linearized by calculating  $E_n$   
 $= \ln (A_n/A_0)$ .

Imaging of thick and thin partitions is feasible:

- 25 (a) all spins in the lung are equally excited.  
 This greatly simplifies matters and is to be  
 preferred in practical applications. In this  
 case, the effect of gas exchange is rendered  
 unobservable, i.e.  $(P - P') \approx 0$  for all times.  
 Experimentally, it can be achieved either by

- 19 -

use of thick slices in 2D techniques, or by 3D acquisitions covering the entire inhaled volume of  $^3\text{He}$ .

- 5 (b) The volume  $V$  of the imaged partition is thin compared to the surrounding volume  $V'$  with which diffusive contact exists within the time scale of a typical imaging sequence. In this case  $\gamma$  and  $\gamma'$  scale according to the ratio of  
10 the volumes involved, hence  $\gamma' = \gamma \cdot V/V'$ . Thus  $\gamma'$  may be neglected if  $V \ll V'$ .

The idea of double acquisition imaging is best illustrated by a simple example.

- 15 Consider a set of images with a single thick slice (i.e. suppressing diffusion effects). If images are taken in equidistant interscan times (hence,  $t_n = n \cdot \tau$ ):

$$E_n = - \int_0^{\tau} \Gamma_{O_2}(t) dt + N n \ln (\cos \alpha) \quad [14]$$

#### Method 1

- 20 The second set of images is acquired retaining  $\tau$ , but doubling  $\alpha$ . Assuming  $p_{O_2}$  and its time development to be equal in a given ROI during both series, the  $E_n$  values of corresponding images can be subtracted giving

$$\frac{E_n(\alpha) - E_n(2\alpha)}{N} = n \ln \left( \frac{\cos \alpha}{\cos 2\alpha} \right) \quad [15]$$

- 25 If the left hand side of [15] is plotted against  $n$ ,  $\ln (\cos \alpha / \cos 2\alpha)$  and furthermore  $\alpha$  are obtained from the slope. In a second step, eq. [14] of either dataset is corrected for flip angle effects, and  $\Gamma_{O_2}$  is extracted by a fit.

#### Method 2

- 30 The second set of images is acquired with the same

- 20 -

RF amplitude, but with a different  $\tau$ . In this case, subtraction of corresponding  $E_n$  values results in elimination of the  $(\cos \alpha)$  term in eq. [14]:

$$\xi.(E_n(\tau_1) - E_n(\tau_2)) = \int_0^{\tau_2} p_{O_2}(\tau) d\tau - \int_0^{\tau_1} p_{O_2}(\tau) d\tau \quad [16]$$

Thus, information about the temporal development of  $p_{O_2}$  is obtained. By correcting eq. [14] for this relaxation effect, depolarization by RF excitations can be computed.

### Example 2

10

Wall relaxation by lung tissue is negligible. The effect of wall relaxation was measured in a deoxygenized lung of a dead pig by double acquisition sampling with varied flip angles (method 1). Immediately after inducing cardiac arrest, oxygen was washed out by ventilating with pure nitrogen for about 15 mins. Subsequently, two series of 11 images each were taken, with RF amplitudes  $U_{RF} = 10V$  in the first and  $U_{RF} = 5V$  in the second series. Partition thickness was 120 mm in coronal orientation in order to excite  $^3He$  spins in the entire lung volume. Interscan time  $\tau$  was 7 secs. A ROI of 415 pixel ( $6.5 \text{ cm}^2$ ) within the cranial left lung was examined. A time constant of longitudinal relaxation  $T_1 = 261(4)$  secs was fitted to the data.

25

This is in accordance with a possible residual oxygen concentration of about 10 mb. The value should thus be understood as a lower limit of wall relaxation time. Assuming wall relaxation only, lung tissue shows a cm/hour rate of at least  $1/22 \text{ cm/hour}$  (assuming spherical alveoles with radius  $r = 200 \mu\text{m}$ ). This value is smaller than that of most bare glass surfaces (see Heil et al., in Phys.Lett. A 201 337 (1995)). It means that non-diseased broncho-alveolar surfaces contain practically no radicals nor other paramagnetic centers.

30

Example 3

One anaesthetized pig (27 kg) was normoventilated inside a MRI unit (Siemens Vision scanner with B = 1.5 T, equipped with one of two transmit/receive coils resonant to  $^3\text{He}$  at 48.44 MHz). After administering a  $\approx 100 \text{ cm}^3$  bolus of  $^3\text{He}$ , two series of 2D FLASH (TE < 4 ms, TR 11 ms), images in transversal orientation were taken during breathhold. Predefined RF excitation intensities U were 10 and 20 Volts and intervals  $\tau$  of 1.5s were used. Partition thickness was 20 mm. Signal intensities were averaged and analyzed over regions of interest (ROIs). An intensity correction for noise was performed following Gudbjartsson et al. MRM 34: 910-914 (1995). A first postprocessing was performed calculating  $E_n = \ln(A_n/A_0)$  for both series, where "ln" denotes the natural logarithm function. Following the dependence

$$D_{(n)} \equiv \frac{E_n[10V] - E_n[20V]}{N} = n \ln \left( \frac{\cos \alpha}{\cos 2\alpha} \right) \quad [17]$$

Figure 6 shows a linear graph (N total number of images taken, n the considered image number). Solving equation (17) one determines the flip  $\alpha = 3.4^\circ$ . Knowing this value, one can fit the signal intensity evolution with the image number given in Figure 7. A linear dependency of the regional partial oxygen pressure proved by other experiments is assumed:  $p(t) = p_0 - mt$  with time t, coefficient m and pressure  $p_0$  at the beginning of the measurement. By method 1,  $[\text{O}_2] = 0.108(3)$  amagat and its change with time by  $m = 0.0026(5)$  amagat/s are extracted (see Figure 8).

Two more theoretical curves indicate the temporal evolution, if no change of partial oxygen pressure takes place ( $m = 0$  amagat/s,  $p_0 = 0.108$  amagat) and if no

- 22 -

relaxation by oxygen would be present ( $m = 0$  amagat/s,  $p_o = 0$  amagat). Both curves indicate, the significant change of partial oxygen pressure. The low value for regional  $p_o$  found seems to be real from comparison with other analyses which yield the same flip angles for such excitation intensities.

#### Example 4

In this example, we present an example of *in vivo* oxygen determination, as obtained from double acquisition with varied interscan time  $\tau$  (method 2). An anaesthetized pig underwent controlled ventilation with room air (oxygen concentration 21%). After  $^3\text{He}$  bolus injection, a series of 8 images with  $\tau_1 = 7$  s was acquired during inspiratory apnea ( $\approx 50$  s). After a short interval to ensure stability of vital parameters, a second series of 8 images with  $\tau_2 = 1$  s was taken. RF amplitude was 10 V in both series, partition thickness was 120 mm in coronal orientation.

The oxygen density  $\rho_{O_2}(t)$  is determined from the sequence of normalised logarithmic intensities  $E_1, E_2 \dots E_n$ . The procedure is simplified if it is assumed a priori that the time dependence of  $\rho_{O_2}$  be linear

$$\rho_{O_2}(t) = \rho_o - Rt, \quad [18]$$

where  $R$  is the rate of oxygen decrease.

One then computes

$$y_n = \xi \frac{E_n(\tau_1) - E_n(\tau_2)}{n(\tau_2 - \tau_1)} = \rho_o - R \left( \frac{n}{2} (\tau_1 + \tau_2) \right) \quad [19]$$

Comparison with eq. [18] shows that the experimental quantities  $y_n$  just equal the searched for oxygen density



- 23 -

$$Y_n = \rho_{O_2}(t_n) \quad [20]$$

at mean times  $t_n = n(\tau_1 + \tau_2)/2$ .

5       The time course of  $\rho_{O_2}(t_n)$  was obtained via eq. [20]  
within a ROI in the middle section of the right lung  
which comprises 89 pixel and covers an area of 1.39 cm<sup>2</sup>.  
A linear decrease of  $\rho_{O_2}$  with time was observed, thus  
confirming the assumption a posteriori.

10       A linear fit to the data yields  $\rho_o = 0.168(5)$  amagat  
and  $R = 0.0034(2)$  amagat/s with a  $\chi^2$  of 1.00 p.d.f.  
Consistent with physiology, the initial oxygen  
concentration is found to be lower in the functional  
residual capacity (FRC) of the lung than in inspired  
air.

15       Once the temporal evolution of  $\rho_{O_2}$  is determined,  
the flip angle  $\alpha$  remains the only unknown parameter in  
eq. [8a]. Considering the uncertainties of intensities  
as statistical and those of  $\rho_o$  and  $R$  as additional  
systematic errors, the  $\tau = 1s$  series yields  $\alpha = 3.36$   
20       (10)° and the  $\tau = 7s$  series  $\alpha = 3.1(3)$ °.

Example 5Effects of Gas Transport Phenomena in the lung on the MR Signal

5

According to eq. [14], the dynamics of intrapulmonary  $^3\text{He}$  polarization are changed significantly when diffusive and/or convective gas transport is taken into account. This is necessarily the case when the imaged partition is thin compared to the total lung volume. In this example, a 20mm slice of a porcine lung was imaged in transversal orientation. Images were taken after cardiac arrest to ensure a time-constant  $\rho_{\text{O}_2}$  (i.e.  $m = 0$ ). The inspiratory oxygen concentration was set to  $(30 \pm 1)\%$ . Two series of nine images each were acquired with RF amplitudes of 10 and 20 V respectively. Interscan delays  $\tau$  were alternating 1.2s and 1.8s. A ROI of 510 pixel, placed in the left lung, was analyzed in this example.

20

The procedure in this case is as follows. As long as the polarization difference  $P-P'$  between the imaged partition and non-imaged surrounding is small, the effect of gas exchange is considered negligible, hence  $P-P' \approx 0$  is approximated in the first three images. Thus,  $\alpha$  and  $\rho_0$  are computed in the same way as in example 3. Using  $\gamma=0$  and linear fitting of subtracted logarithmic intensities  $E_n$  ( $n=0,1,2$ ), we obtain a flip angle  $\alpha = 2.9(1)^\circ$  for 10 V excitation. Subsequently, flip angle corrected intensities of these first images are fitted to determine  $\rho_0 = 0.31(2)$  amagat. In a third step, the entire dataset of one acquisition is utilized to fit  $\gamma$  according to eq. [14].

30

Fig. 9 depicts the signal intensities  $A_n(U_{\text{RF}}=10 \text{ V})$  as a function of time. The upper curve refers to a fit with  $\Gamma_{\text{RF}}=0.070\text{s}^{-1}$  and  $\rho_{\text{O}_2}=\rho_0=0.31$  amagat as input parameters. The fit yields  $\gamma=0.056(26)\text{s}^{-1}$ . Also shown is a curve for identical flip angle and oxygen

35

- 25 -

concentration, but with  $\gamma=0$ . Clearly this curve tends to increasingly disagree with the data points after about 5s, whereas only a small discrepancy is detected for the first three images, justifying the said method of analysis.

#### Example 6

#### Determination of Oxygen Concentration using a Single Acquisition

In this example the imaged object was a rubber bag of volume 0.5 liters. An application of  $^3\text{He}$  bolus 0.1 l, flushed by 0.4 l of air ( $\text{O}_2$  concentration 21%) was performed.

The imaging was performed on (Siemens Vision Scanner with  $B=1.5$  T equipped with transmit/receive coil resonant to  $^3\text{He}$  at 48.44 MHz) using a 2D Flash sequence, partition thickness 12 cm, covering entire volume of bag.

Parameter variation was realized with one single imaging sequence, permitting quantification of flip angle and oxygen concentration.

7 images were taken with  $U_{\text{HF}}=5$  V, interscan time 2.6s. Thereafter, 6 images were taken with  $U_{\text{HF}}=20$  V, interscan time 1s.

Flip angle was determined from a fit of intensities of a ROI of the last 6 images, "guessing" an initial oxygen concentration. Obtained result was used to compute  $[\text{O}_2](t)$  from a fit of intensities of a ROI of the first 7 images. Accuracy was improved by iterating this process 2 times.

Results: flip angle  $\alpha$  was determined to be  $4.40(7)^\circ$  for 20 V excitation.

Oxygen concentration was determined to 0.186(7) amagat, consistent with  $\text{O}_2$  concentration in room air.

Since a phantom was imaged, no decrease of oxygen

- 26 -

was observed, see Fig. 10.

#### Example 7

##### 5    A First Oxygen Determination Routine using Variation of 10   Low Flip Angle

Hyperpolarized  $^3\text{He}$  ( $^3\text{He}$ ) is described as non-  
radioactive inhalational contrast agent for magnetic  
10   resonance (MR) tomography of ventilated lung spaces. In  
 $^3\text{He}$ -MRI, signal intensity is destroyed irrecoverably by  
(1) the presence of paramagnetic oxygen in the  
respiratory gas and (2) MR image acquisition itself.  
Regional intrapulmonary  $[\text{O}_2]$  as a sum of inspiratory  
15   oxygen concentration ( $\text{F}_\text{I}\text{O}_2$ ), distribution of ventilation,  
and oxygen uptake is determined in clinical practice  
globally over the whole lung. The aim was to use the  
effect of oxygen upon  $^3\text{He}$  to visualise regional  
intrapulmonary  $[\text{O}_2]$  in MR for the first time on a  
20   regional basis.

**Animal and Methods:** Eight anesthetized healthy  
pigs ( $28 \pm 2$  kg) were normoventilated in a 1.5 T MRI unit  
fitted with a Helmholtz transmit-receive coil tuned to  
48.4 MHz. Hemodynamic parameters and end-tidal  $[\text{O}_2]$  were  
25   measured continuously.

Interventions included variation of  $^3\text{He}$  bolus sizes,  
of RF amplitudes for MR-image acquisition (10V and 20V),  
of end-tidal  $[\text{O}_2]$  (0.16, 0.25, 0.35 and 0.45), and  
comparison of intrapulmonary  $[\text{O}_2]$  before and after  
30   induction of cardiac arrest.

Using a dedicated application unit specifically  
designed by our group, see PCT/EP98/07516 (copy filed  
herewith), boli of  $^3\text{He}$  (up to 45% polarized) were  
administered at the beginning of inspiratory tidal  
35   volumes. During subsequent inspiratory apnea, serial  $^3\text{He}$   
images of airways and lungs were acquired using a two-  
dimensional FLASH sequence (image acquisition time = 1

- 27 -

s; TR = 11 ms/TE = 4.2 ms; 1.5 s inter-image delay).

The decay of MR signal intensities in various regions of interest within pulmonary cross-sections was analysed with respect to the different interventions.

5 RF excitation effects upon signal intensity decay were separated from oxygen effects by comparison of image series acquired with two different flip angles  $< 7^\circ$ .

**Results:** Single-breath, single-bolus  $^3\text{He}$  administration allowed reproducible visualization of  
10 airways and lungs. Bolus volumina between 20 mL and 100 mL could be administered reproducibly (40 mL:  $39 \pm 4$  mL; 100 mL:  $100 \pm 4$  mL;  $n=25$ ). Images containing regions with a signal-to-noise ratio  $> 3$  were required for analysis of the signal decay function; this could be  
15 achieved in up to 10 subsequent images following a single  $^3\text{He}$  bolus.  $T_1$  of hyperpolarized  $^3\text{He}$  demonstrated a similar relationship to ambient  $[\text{O}_2]$  as had been found *in vitro*. Signal analysis within two consecutive images, which were acquired at a known  $F_{\text{et}}\text{O}_2$ , allowed  
20 determination of polarization loss due to MR acquisition (for 10V or 20V, respectively). Taking this effect into account, the analysis of independently acquired image series yielded estimates for regional  $[\text{O}_2]$ . Analysis of MR signal decay in defined ROIs of two-dimensional  $^3\text{He}$   
25 images yielded values for regional intrapulmonary  $[\text{O}_2]$  which correlated closely with end-expiratory  $[\text{O}_2]$  ( $r = 0.94$ ;  $p < 0.001$ , Figure 4) before induction of cardiac arrest, and with inspiratory oxygen concentration during absence of perfusion.

30 **Conclusions:** This study demonstrates a) reproducible visualization of small quantities of  $^3\text{He}$  in the lungs, b) *in vivo* confirmation of the oxygen- $T_1$  relationship described by Saam et al. in Phys.Rev. **A52**, 862 (1995), c) feasibility of non-invasive MR-based  
35 analysis of regional intrapulmonary  $[\text{O}_2]$  in a range of oxygen concentrations which is used in ventilator-dependent patients, and d), significant correlation of

- 28 -

<sup>3</sup>He-MR-determined with measured end-expiratory oxygen concentrations. As hyperpolarized <sup>3</sup>He can be distributed in special glass cells (half-time of hyperpolarization > 80 h), and technical requirements are limited to a spectroscopy option for the used MR scanner and a dedicated <sup>3</sup>He-coil, early propagation of this method is expected. The new technique may provide insight into regional O<sub>2</sub> exchange in the lungs. Further human and animal studies are necessary to demonstrate the spatial and temporal resolution in the analysis of O<sub>2</sub> distribution and exchange under pathological conditions by this non-invasive new technique.

Figure 5 shows the analysis of the time course of oxygen concentration in the lung of a male volunteer, analysed with the double acquisition method with variation of flip angle as described in the present example above. Initial oxygen concentration at the beginning of the breathhold (0.189) and calculated oxygen decrease during apnea (0.01/s) can be followed.

#### Example 8

<sup>3</sup>He gas was hyperpolarized to approximately 40-50% by optical pumping. 12 volunteers and 10 pneumologic patients inhaled such gas from glass cylinders of 300 mL volume and 3 bar pressure. <sup>3</sup>He-MRI was performed during breathhold using a 3D gradient-recalled-echo imaging sequence on a Siemens 1.5T clinical scanner, adjusted to have a transmitter frequency of 48.4 MHz and using a Helmholtz transmit/receive RF coil. A flip angle less than 5° was used.

In quantitative studies, faster, repeated 3D images (TR=5ms, TE=2ms) were acquired at intervals of 0.8, 16, 42 and 55 seconds in normal volunteers. From these 5 images, extraction of both regional flip angle and regional T<sub>1</sub> was possible defining the effects of repeated RF pulsing and longitudinal relaxation in terms of decay

- 29 -

rate constants,  $\Gamma_{RF}$  and  $\Gamma_{RELAX}$  respectively. For a pulse train of duration  $T$ , consisting of  $N$  pulses of flip angle  $\phi$ ,  $\Gamma_{RF}$  is given by:

5 
$$\Gamma_{RF} T = [\cos(\phi)]^N \quad (15)$$

On the other hand, the contribution of longitudinal relaxation depends on absolute time, not on the duration of the RF pulsing. Thus by using a non-linear image  
10 timing sequence, the two effects can be resolved and both flip angle and  $T_1$  determined regionally.

A final study, using an ultrafast 2D sequence, generated images every 1 second during inspiration, breathhold and expiration.

15 **Results:** All volunteers and 8/10 patients were able to perform the necessary inhalation. One patient was claustrophobic and 1 patient could not maintain a 25-second breathhold. The central airways were consistently visualized. Volunteers demonstrated  
20 homogeneous signal intensity; patients with obstructive lung disease and/or pneumonia demonstrated characteristically inhomogeneous signal intensities, specific for the disorder.

Flip angle calibration confirmed an estimated flip  
25 angle of 1-2°.  $T_1$  was derived to be 32±3 seconds in normal lung. In phantoms, longitudinal relaxation was negligible compared with RF pulsing over a time period of 1 minute (this is consistent with predicted  $T_1$  values of tens of hours).

30 Using the rapid 2D sequence, the inspiratory process could be seen to have a timecourse of less than 1s in normal lung (providing 'instantaneous' uniform signal). Expiration gave rise to slower signal change. The signal reducing effect of expiration could be  
35 clearly discriminated from the continuing destruction of polarization by RF pulsing, allowing estimation of lung residual volume.

- 30 -

**Conclusion:**  $^3\text{He}$ -MRI with inspiration of hyperpolarized  $^3\text{He}$  provides a means of imaging lung ventilation. Lung filling and ventilatory obstruction can be examined with dynamic MRI. Quantitation, particularly of regional  $^3\text{He}$   $T_1$ , provides a means of assessing local physiologic parameters, such as  $p\text{O}_2$ . The simple quantitative approaches described in this Example slow  $^3\text{He}$ -MRI of the lung provides a modality capable of providing regional functional and physiological information.

#### Example 9

##### Ultrafast Ventilation Scan

**Material and methods:** Coronal images of the lung were acquired at 48.44 MHz using ultrafast gradient-echo pulse sequence with  $TR/TE/\alpha=2.0\text{ms}/0.7\text{ms}/1.5^\circ$ . A series of 160 projection images was obtained with 128ms temporal resolution. Imaging was performed before, during and after application of a single bolus of approximately 300ml  $^3\text{He}$  in five healthy volunteers (spontaneous breathing). The signal intensities were corrected for depolarisation by RF excitation on the basis of equation (5) of this invention. Images from a healthy volunteer at time 0s, 0.13s, 0.26s, 0.65s, 1.17s, 1.95s, 3.77s and 6.37s after inspiration of a single bolus (285 mL) hyperpolarized Helium-3 are shown in Figure 11. Figure 12, meanwhile, shows signal-time-curves in trachea and in parenchyma on the right side of the lung in the patient of Figure 11. Shaded areas denote intervals of expiration (determined from the diaphragm position), interrupted by intervals of inspiration (not shaded). During the first phase of inspiration,  $^3\text{He}$  signal appears in the trachea. It reappears during the expiratory cycles. After a delayed signal increase in alveolar space,  $^3\text{He}$  signal decreases



- 31 -

there due to  $T_1$  relaxation, depolarisation by RF pulses, and due to expiration and inspiration with air.

**Results:** In these gradient recalled images no susceptibility artifacts are observed. Distribution of the  $^3\text{He}$  boli was observed in the trachea, in mainstem and distal bronchi down to fourth order, and in alveolar space. The temporal resolution was 130 ms, spatial resolution was 2.5mm x 4.4mm. The signal of a single bolus of  $^3\text{He}$  was detected in the lung for up to 20s. The peak signal-to-noise ratio in the lung was  $11.7 \pm 7.7$ . While the time-to-peak of the bolus signal in the trachea was 260ms, it was significantly longer in lung parenchyma (910ms).

**Conclusion:** Individual phases of inspiration, distribution of  $^3\text{He}$  within the alveolar space and expiration can be visualized by ultrafast imaging of a single bolus of hyperpolarized  $^3\text{He}$  gas. This method may allow for regional analysis of lung function with temporal and spatial resolution superior to conventional methods.

- 32 -

Claims

1. A method of detecting regional variations in oxygen uptake from the lungs of an air-breathing animal  
5 subject, said method comprising administering into the lungs of said subject a diagnostically effective amount of a gaseous hyperpolarized magnetic resonance imaging agent, detecting the magnetic resonance signal from said agent in said lungs, determining the temporal variation  
10 in relaxation rate for said signal for at least one region of interest within said lungs, and from said variation generating a qualitative or quantitative value or image indicative of the oxygen concentration in at least one region of interest, and if desired the time  
15 dependency of such concentration.
2. A method as claimed in claim 1 wherein said hyperpolarized agent comprises  $^3\text{He}$ .
- 20 3. A method as claimed in claim 1 wherein detection of said magnetic resonance signal is effected during a period of at least 1 second during which there is substantially no gas flow into or out of the lungs.
- 25 4. A method as claimed in claim 1 wherein said regions of interest comprise regions of alveolar space.
5. A method as claimed in claim 1 wherein a temporal and/or spatial mr image of at least part of the lungs  
30 comprising said regions of interest is also generated.
6. A method as claimed in claim 5 wherein said temporal and/or spatial image is constructed from magnetic resonance signals from said hyperpolarized  
35 agent.
7. A method as claimed in claim 5 wherein said

- 33 -

temporal and/or spatial image is constructed from magnetic resonance signals from magnetic resonance active nuclei in a further magnetic resonance imaging agent administered into the vasculature or lungs of said  
5 subject.

8. A method as claimed in claim 7 wherein said further agent comprises a  $^{19}\text{F}$  fluorocarbon.

10 9. A method as claimed in claim 1 wherein said magnetic resonance signals are detected in at least two different types of magnetic resonance imaging sequence.

15 10. A method as claimed in claim 9 wherein said types of sequence differ in the intensity of the magnetic resonance signal stimulating radiation.

20 11. A method as claimed in claim 9 wherein said types of sequence differ in the sequence timing.

12. A method as claimed in claim 9 wherein said types of sequence are interleaved.

25 13. A method as claimed in claim 1 wherein magnetic resonance signal detection is effected in an imaging sequence with an image acquisition time of less than 2 seconds.

30 14. A method as claimed in claim 1 wherein magnetic resonance signal detection is effected in an imaging sequence involving imposition of a flip angle of less than  $7^\circ$ .

35 15. A method as claimed in claim 1 wherein said hyperpolarized agent is administered as a bolus.

16. A method as claimed in claim 1 wherein said

- 34 -

hyperpolarized agent is administered as a bolus of volume 1 to 1000 ml.

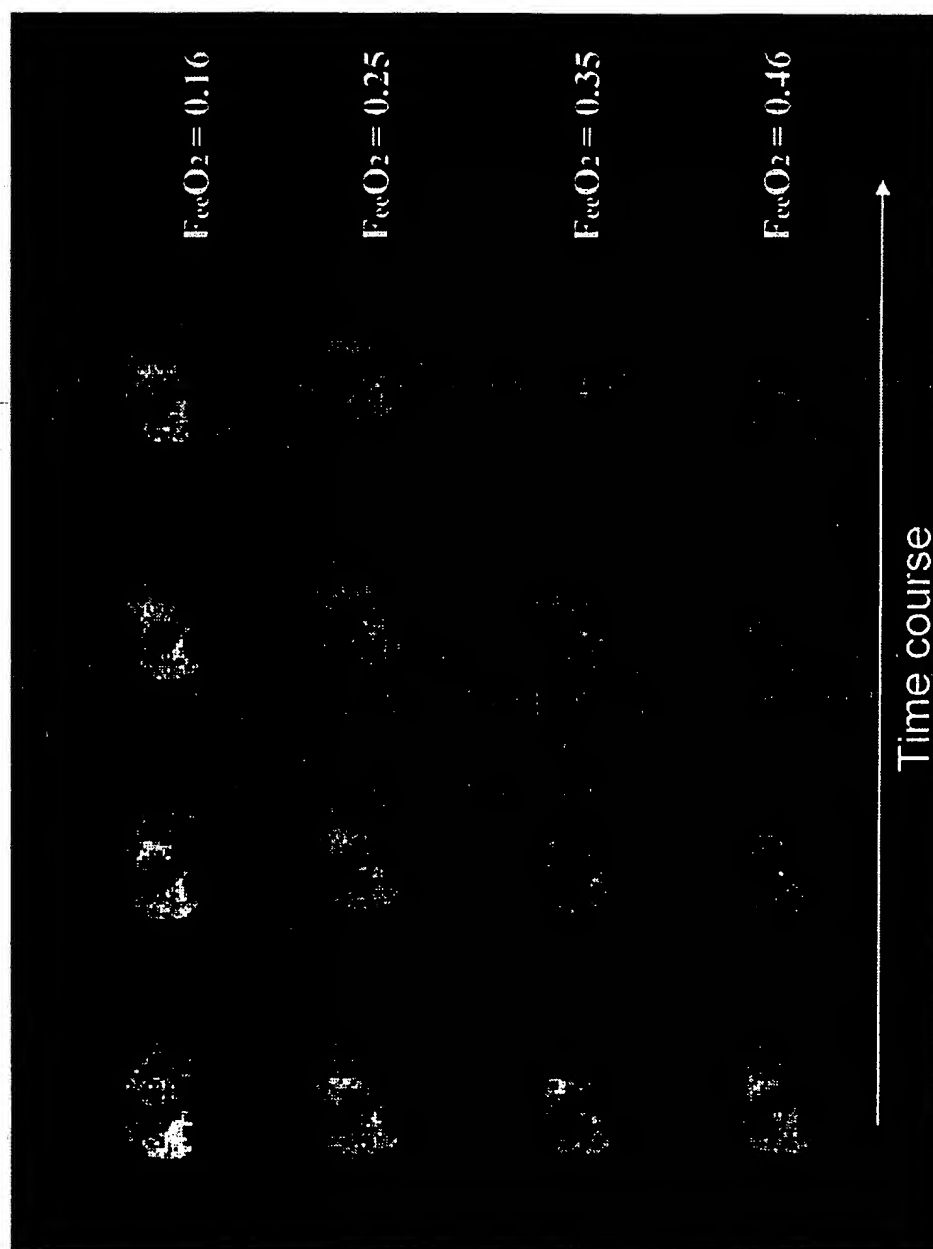
5 17. A method as claimed in claim 1 wherein a mr imager with a primary field strength in the range of 0.05 to 8T, preferably 0.05 to 3.5T, is used to detect said magnetic resonance signal.

10 18. A method as claimed in claim 1 wherein said hyperpolarized agent comprises  $^{129}\text{Xe}$ .

15 19. A method as claimed in any one of the preceding claims wherein the acquisition time of said image is in the subsecond range.

20 20. A method as claimed in any one of the preceding claims wherein said image is produced by any method selected from the group of gradient-recalled-echo imaging, echo-planar imaging, turbo-spin-echo imaging and imaging based on projection techniques.

21. A method as claimed in any one of the preceding claims allowing determination of functional residual capacity, dead space and regional ventilation.



Time course

FIG. 1A

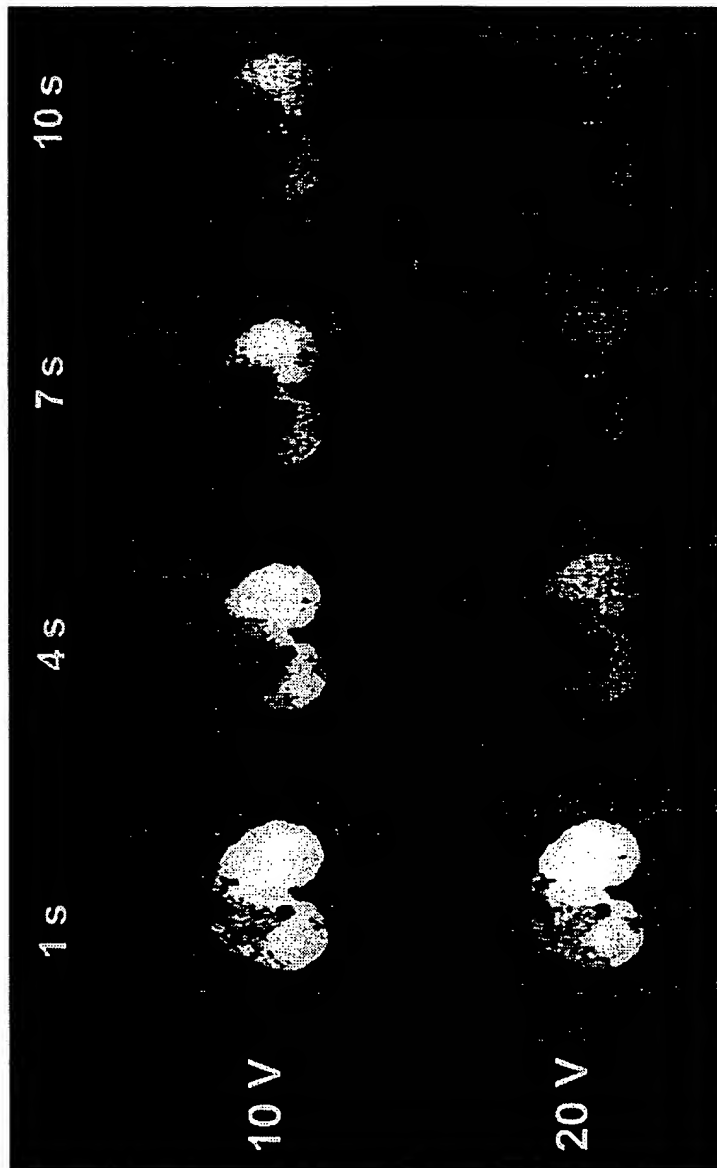


FIG. 1B

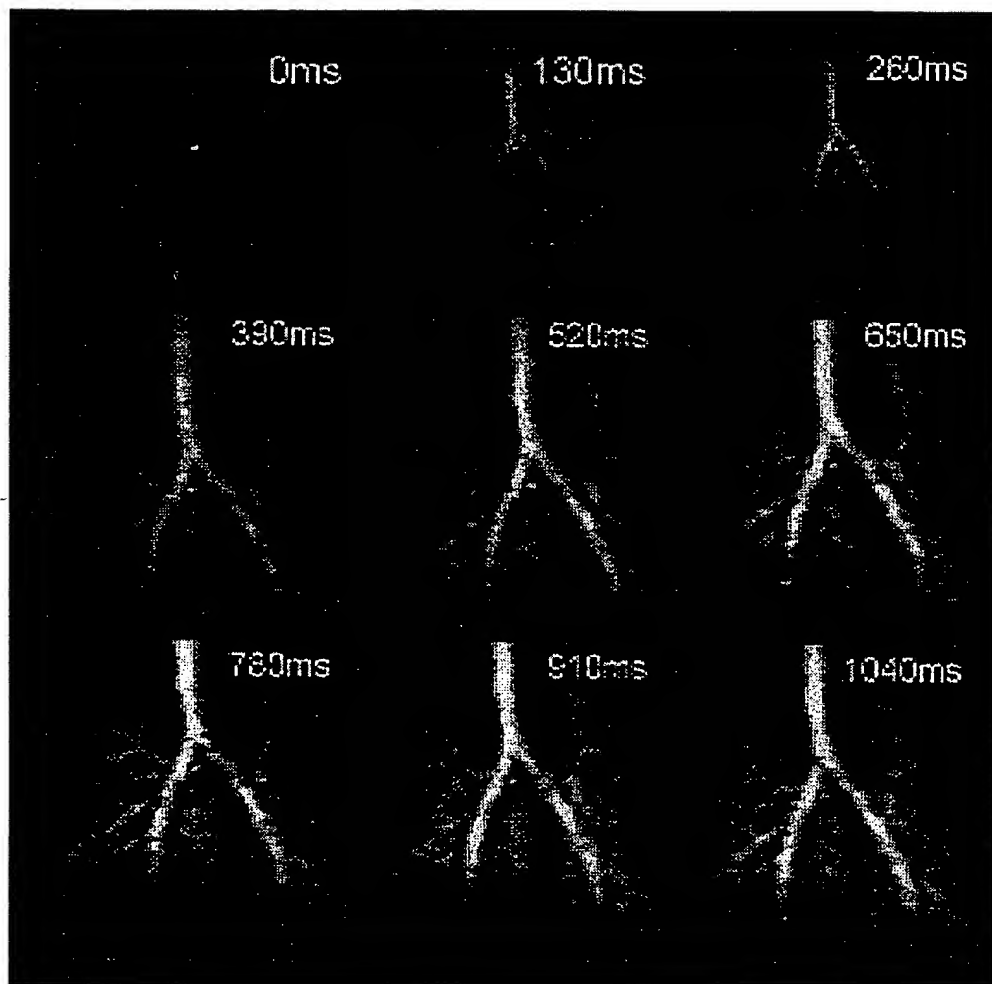


FIG. 2

4 / 13

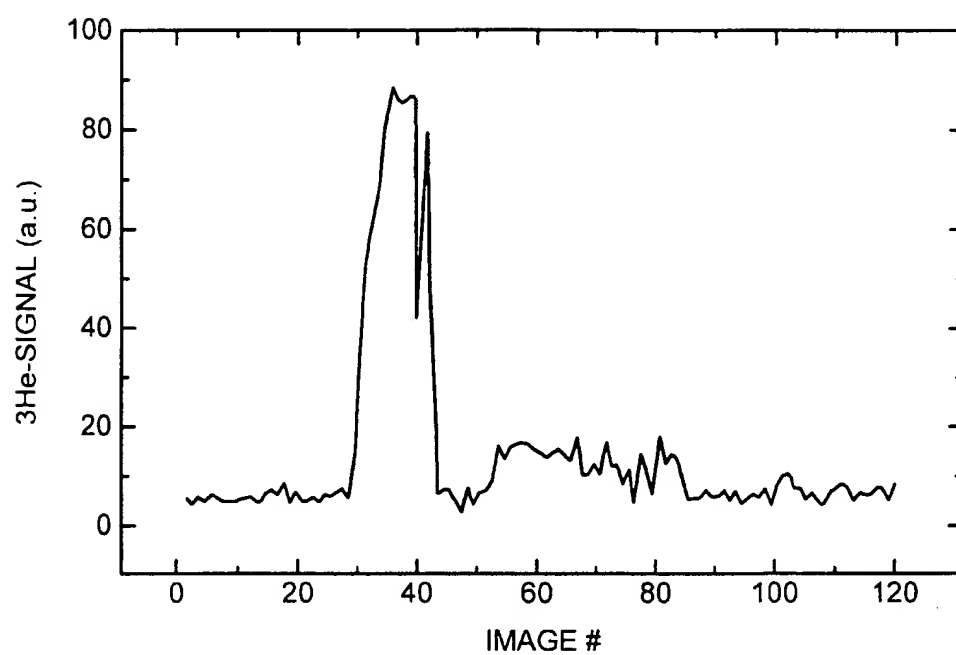


FIG. 3



5 / 13

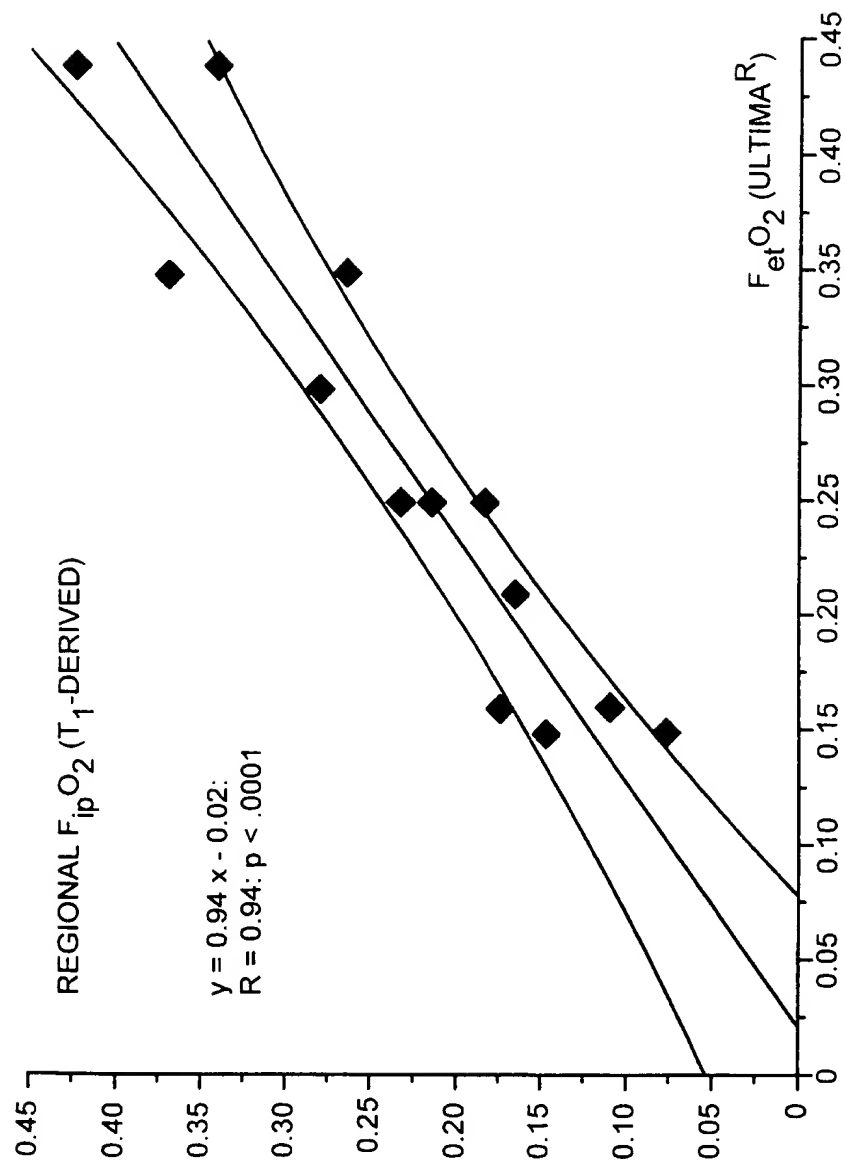


FIG. 4

6 / 13

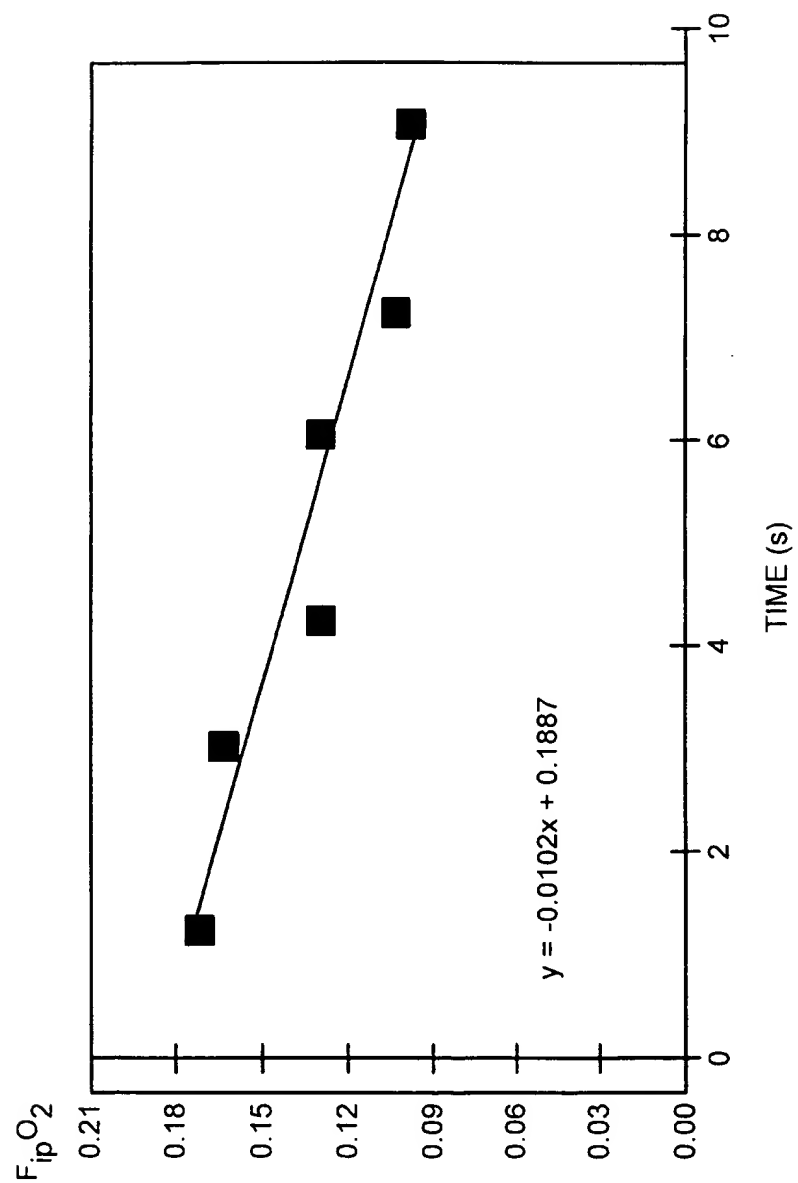


FIG. 5

7 / 13

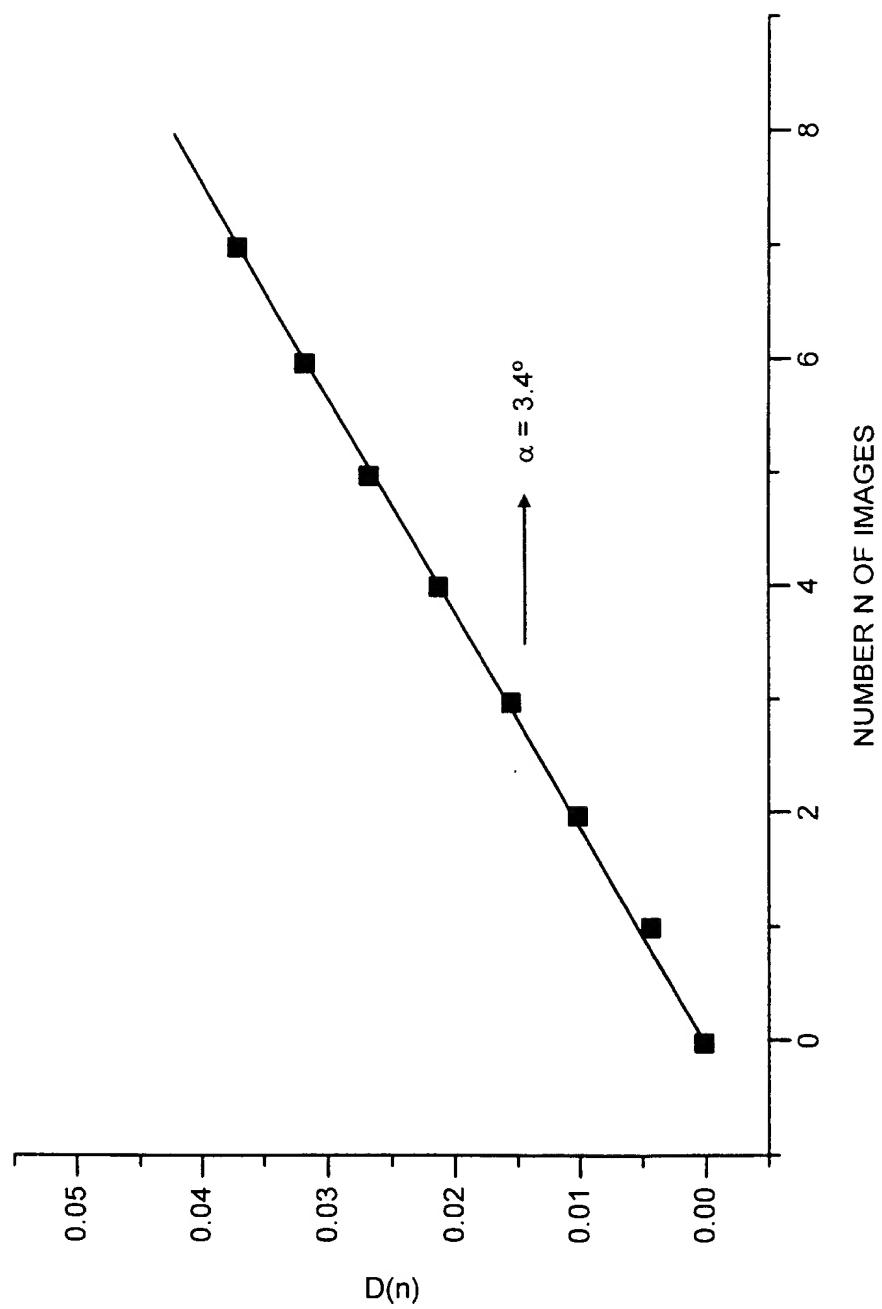


FIG. 6

8 / 13

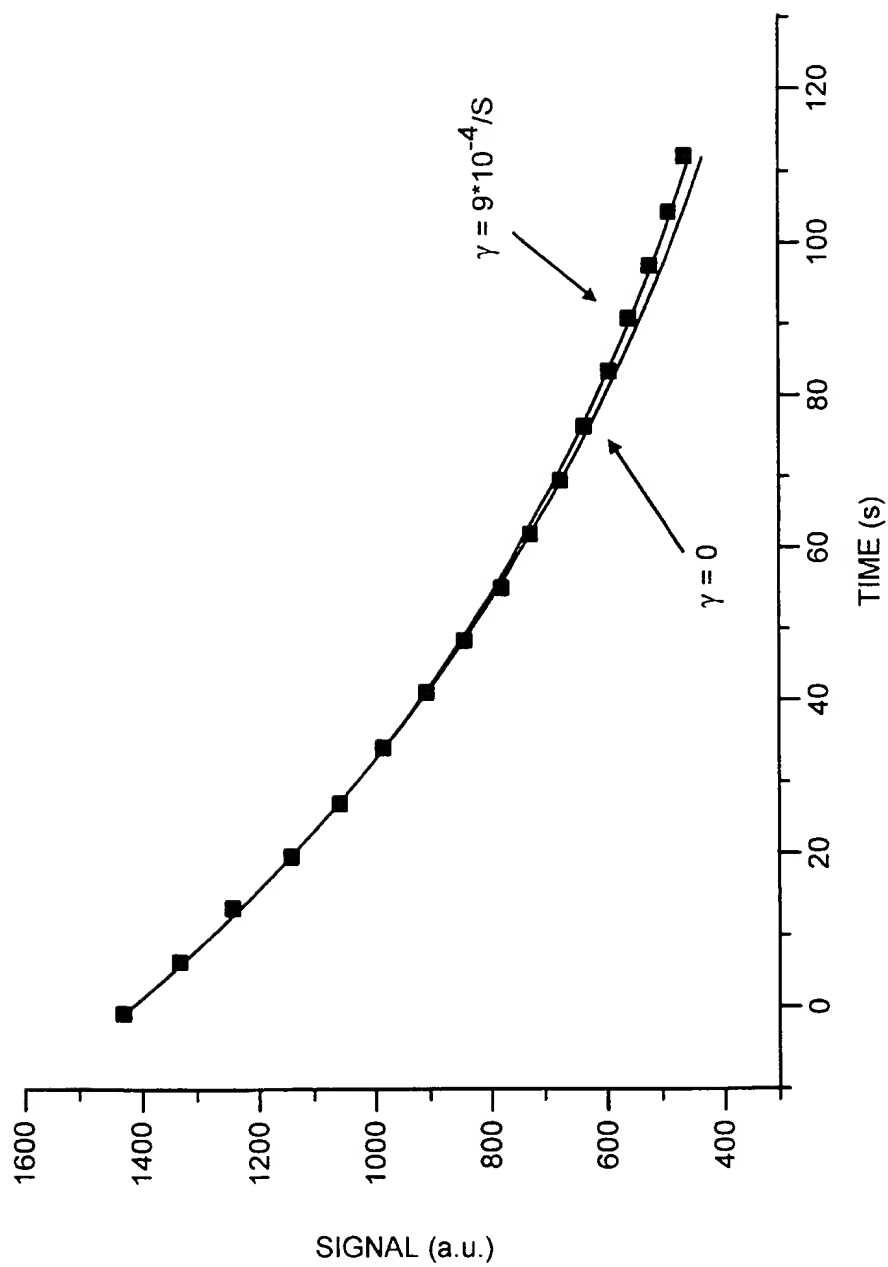


FIG. 7

9 / 13

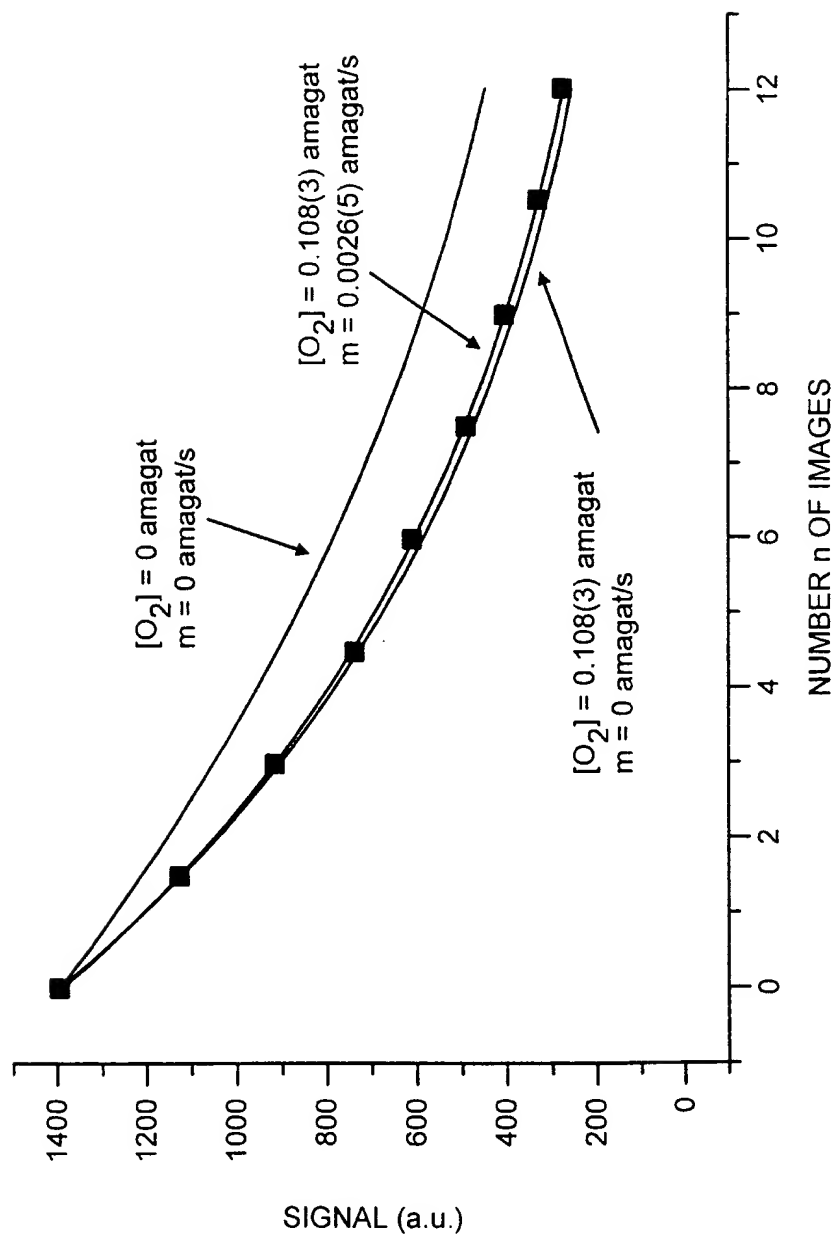
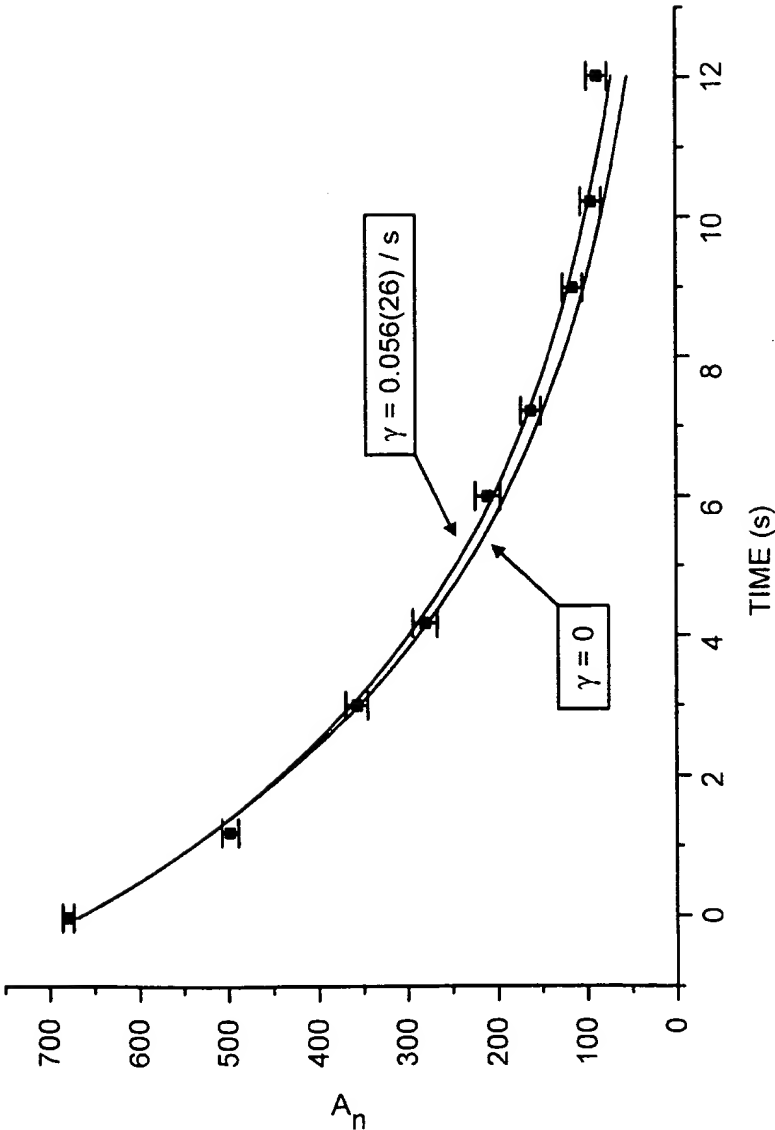


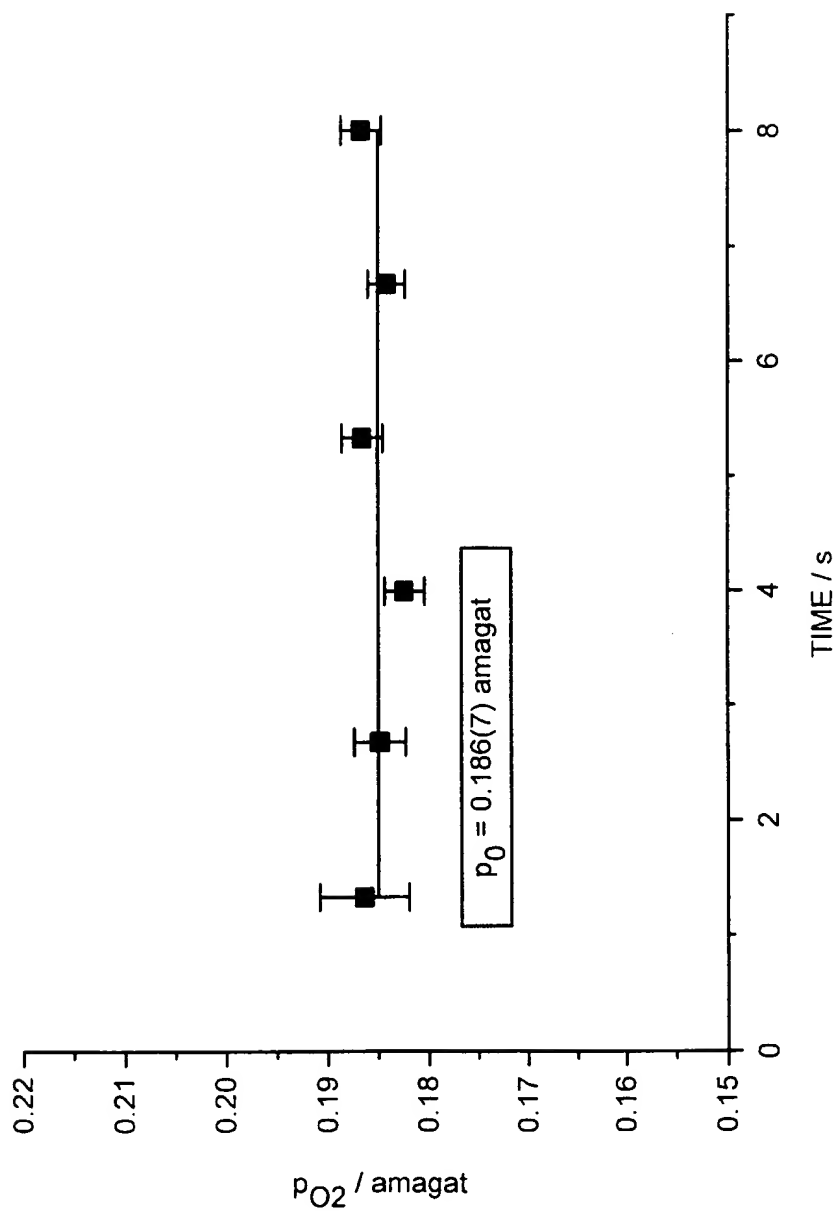
FIG. 8



DETERMINATION OF GAS TRANSPORT PARAMETER  $\gamma$ . FLIP ANGLE AND OXYGEN CONCENTRATIONS ARE EVALUATED BEFOREHAND AND USED AS INPUT PARAMETERS HERE. ALSO SHOWN IS A THEORETICAL CURVE WITH SAME  $\alpha$  AND  $p_{O_2}$ , BUT WITH  $\gamma = 0$ .

FIG. 9

11 / 13



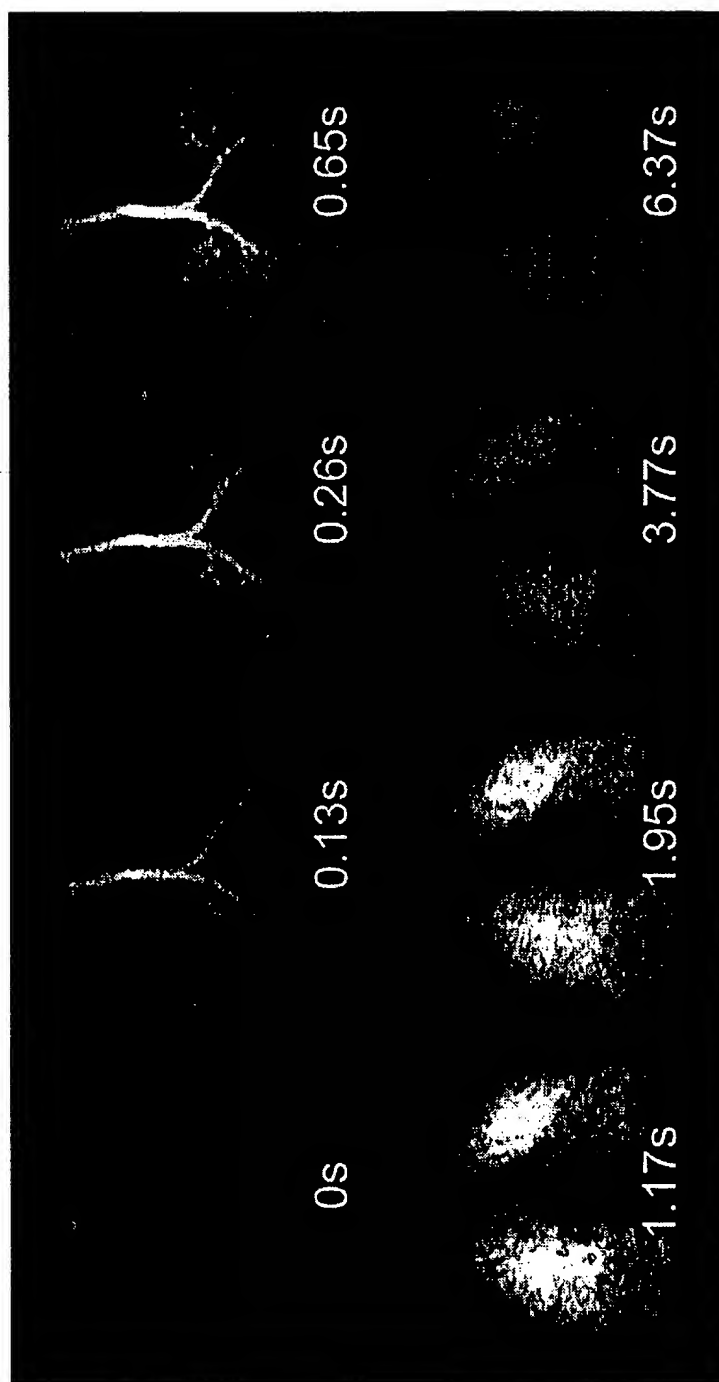


FIG. 11



13 / 13

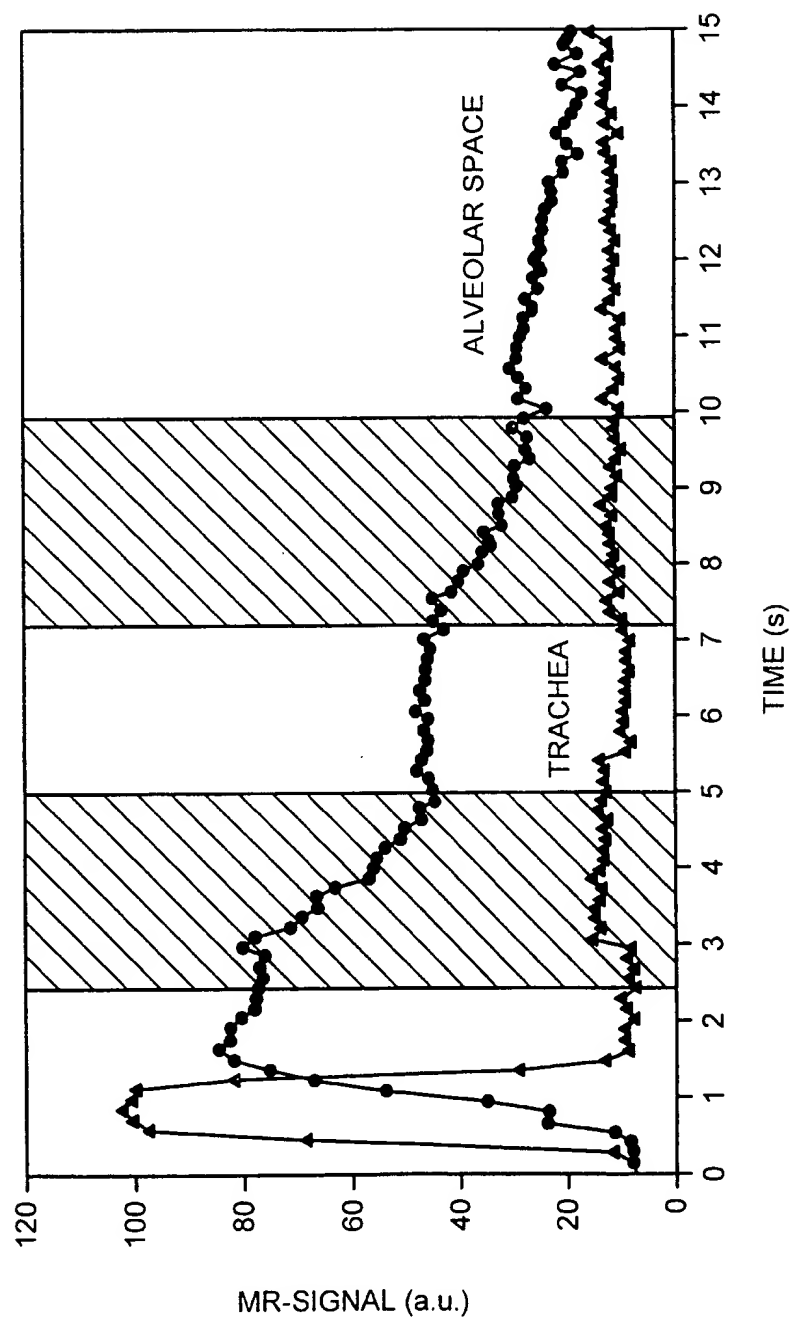


FIG. 12

# INTERNATIONAL SEARCH REPORT

Int. :ional Application No

PCT/GB 99/01095

A. CLASSIFICATION OF SUBJECT MATTER  
IPC 6 G01R33/28

According to International Patent Classification (IPC) or to both national classification and IPC

## B. FIELDS SEARCHED

Minimum documentation searched (classification system followed by classification symbols)

IPC 6 G01R

Documentation searched other than minimum documentation to the extent that such documents are included in the fields searched

Electronic data base consulted during the international search (name of data base and, where practical, search terms used)

## C. DOCUMENTS CONSIDERED TO BE RELEVANT

Category *	Citation of document, with indication, where appropriate, of the relevant passages	Relevant to claim No.
P,X	KAUCZOR H -U: "Helium-3 imaging of pulmonary ventilation" BRITISH JOURNAL OF RADIOLOGY, JULY 1998, BRITISH INST. RADIOLOGY, UK, vol. 71, no. 847, pages 701-703, XP002109516 ISSN 0007-1285 see the whole document --- -/--	1-6,9-21



Further documents are listed in the continuation of box C.



Patent family members are listed in annex.

### \* Special categories of cited documents :

- "A" document defining the general state of the art which is not considered to be of particular relevance
- "E" earlier document but published on or after the international filing date
- "L" document which may throw doubts on priority claim(s) or which is cited to establish the publication date of another citation or other special reason (as specified)
- "O" document referring to an oral disclosure, use, exhibition or other means
- "P" document published prior to the international filing date but later than the priority date claimed

- "T" later document published after the international filing date or priority date and not in conflict with the application but cited to understand the principle or theory underlying the invention
- "X" document of particular relevance; the claimed invention cannot be considered novel or cannot be considered to involve an inventive step when the document is taken alone
- "Y" document of particular relevance; the claimed invention cannot be considered to involve an inventive step when the document is combined with one or more other such documents, such combination being obvious to a person skilled in the art.
- "&" document member of the same patent family

Date of the actual completion of the international search

19 July 1999

Date of mailing of the international search report

12/08/1999

Name and mailing address of the ISA

European Patent Office, P.B. 5818 Patentlaan 2  
NL - 2280 HV Rijswijk  
Tel. (+31-70) 340-2040. Tx. 31 651 epo nl,  
Fax: (+31-70) 340-3016

Authorized officer

Lersch, W

# INTERNATIONAL SEARCH REPORT

Int: tional Application No

PCT/GB 99/01095

## C.(Continuation) DOCUMENTS CONSIDERED TO BE RELEVANT

Category	Citation of document, with indication, where appropriate, of the relevant passages	Relevant to claim No.
X	WO 95 27438 A (UNIV NEW YORK ;UNIV PRINCETON (US)) 19 October 1995 cited in the application see page 5, line 25 - page 9, line 36 see page 12, line 4 - page 12, line 19 see page 14, line 29 - page 15, line 18 see page 20, line 4 - page 23, line 33 see page 30, line 14 - page 31, line 9 see page 42, line 14 - page 43, line 28	1,2,4-7, 13-21
Y	---	3,8-12
A	US 4 775 522 A (CLARK JR LELAND C) 4 October 1988 see column 5, line 14 - column 7, line 37 see column 8, line 43 - column 10, line 25 see column 11, line 19 - column 11, line 31	1,5-7, 17,20,21
Y	---	8
Y	PATYAL B R ET AL: "Longitudinal relaxation and diffusion measurements using magnetic resonance signals from laser-hyperpolarized /sup 129/Xe nuclei" JOURNAL OF MAGNETIC RESONANCE, MAY 1997, ACADEMIC PRESS, USA, vol. 126, no. 1, pages 58-65, XP000690998 ISSN 1090-7807 see the whole document	9-12
A	---	1,2
A	SAAM B ET AL: "Nuclear relaxation of /sup 3/He in the presence of O/sub 2/" PHYSICAL REVIEW A (ATOMIC, MOLECULAR, AND OPTICAL PHYSICS), JULY 1995, USA, vol. 52, no. 1, pages 862-865, XP002109517 ISSN 1050-2947 cited in the application	1-6, 13-21
A	---	1-6, 13-21
	ALBERT M S ET AL: "Development of hyperpolarized noble gas MRI" 7TH RCNP INTERNATIONAL WORKSHOP ON POLARIZED /SUP 3/HE BEAMS AND GAS TARGETS AND THEIR APPLICATION, KOBE, JAPAN, 20-24 JAN. 1997, vol. 402, no. 2-3, pages 441-453, XP004107386 ISSN 0168-9002, Nuclear Instruments & Methods in Physics Research, Section A (Accelerators, Spectrometers, Detectors and Associated Equipment), 11 Jan. 1998, Elsevier, Netherlands ---	
	-/--	

# INTERNATIONAL SEARCH REPORT

Int. l. Application No

PCT/GB 99/01095

## C.(Continuation) DOCUMENTS CONSIDERED TO BE RELEVANT

Category	Citation of document, with indication, where appropriate, of the relevant passages	Relevant to claim No.
Y	KAUCZOR H -U ET AL: "Normal and abnormal pulmonary ventilation: visualization at hyperpolarized He-3 MR imaging" RADIOLOGY, NOV. 1996, RADIOL. SOC. NORTH AMERICA, USA, vol. 201, no. 2, pages 564-568, XP002066864 ISSN 0033-8419 see the whole document	3
A		1,2,4-6, 14-18, 20,21
A	----- BERTHEZENE Y ET AL: "CONTRAST-ENHANCED MR IMAGING OF THE LUNG: ASSESSMENTS OF VENTILATION AND PERFUSION" RADIOLOGY, vol. 183, no. 3, 1 June 1992, pages 667-672, XP000674417 -----	7

# INTERNATIONAL SEARCH REPORT

Information on patent family members

International Application No

PCT/GB 99/01095

Patent document cited in search report	Publication date	Patent family member(s)	Publication date
WO 9527438 A	19-10-1995	US 5545396 A	13-08-1996
		AU 2278795 A	30-10-1995
		CA 2183740 A	19-10-1995
		EP 0754009 A	22-01-1997
		JP 10501708 T	17-02-1998
		US 5789921 A	04-08-1998
		US 5785953 A	28-07-1998
US 4775522 A	04-10-1988	US 4586511 A	06-05-1986
		AU 569492 B	04-02-1988
		AU 2504184 A	06-09-1984
		CA 1223037 A	16-06-1987
		EP 0118281 A	12-09-1984
		JP 1896901 C	23-01-1995
		JP 6025074 B	06-04-1994
		JP 59196448 A	07-11-1984